IEEE Transactions on Machine Learning in Communications and Networking

Received 1 December 2023; revised 15 April 2024; accepted 31 May 2024.
Date of publication 5 June 2024; date of current version 13 September 2024.

The associate editor coordinating the review of this article and approving it for publication was M. Chen.

Digital Object Identifier 10.1109/TMLCN.2024.3410211

Decentralized Aggregation for Energy-Efficient Federated Learning in mmWave Aerial-Terrestrial Integrated Networks

MOHAMMED SAIF[1] (Member, IEEE), MD. ZOHEB HASSAN[2] (Member, IEEE), AND MD. JAHANGIR HOSSAIN[3] (Senior Member, IEEE)

[1]Department of Electrical and Computer Engineering, University of Toronto, Toronto, ON M5S 1A1, Canada
[2]Electrical and Computer Engineering Department, Université Laval, Québec, QC G1V 0A6, Canada
[3]School of Engineering, The University of British Columbia, Kelowna, BC V1V 1V7, Canada

CORRESPONDING AUTHOR: M. Z. HASSAN (md-zoheb.hassan@gel.ulaval.ca)

This work was supported in part by the Natural Science and Engineering Research Council of Canada (NSERC) Postdoctoral Fellowship and in part by NSERC Discovery Grant Programs.

ABSTRACT It is anticipated that aerial-terrestrial integrated networks incorporating unmanned aerial vehicles (UAVs) mounted relays will offer improved coverage and connectivity in the beyond 5G era. Meanwhile, federated learning (FL) is a promising distributed machine learning technique for building inference models over wireless networks due to its ability to maintain user privacy and reduce communication overhead. However, off-the-shelf FL models aggregate global parameters at a central parameter server (CPS), increasing energy consumption and latency, as well as inefficiently utilizing radio resource blocks (RRBs) for distributed user devices (UDs). This paper presents a resource-efficient and decentralized FL framework called FedMoD (**fed**erated learning with **mo**del **d**issemination), for millimeter-wave (mmWave) aerial-terrestrial integrated networks with the following two unique characteristics. Firstly, FedMoD incorporates a novel decentralized model dissemination scheme that uses UAVs as local model aggregators through UAV-to-UAV and device-to-device (D2D) communications. As a result, FedMoD 1) increases the number of participant UDs in developing the FL model; and 2) achieves global model aggregation without involving CPS. Secondly, FedMoD reduces FL's energy consumption using radio resource management (RRM) under the constraints of over-the-air learning latency. To achieve this, by leveraging graph theory, FedMoD optimizes the scheduling of line-of-sight (LOS) UDs to suitable UAVs and RRBs over mmWave links and non-LOS UDs to available LOS UDs via overlay D2D communications. Extensive simulations reveal that FedMoD, despite being decentralized, offers the same convergence performance to the conventional centralized FL frameworks.

INDEX TERMS Decentralized FL model dissemination, energy consumption, UAV communications.

I. INTRODUCTION

Unmanned aerial vehicles (UAVs) are expected to have a significant impact on the economy by 2026 with a projected global market value of US$59.2 billion, making the inclusion of UAVs critical in beyond 5G cellular networks [1]. UAV-mounted communication platforms have several unique features, including the high likelihood of establishing line-of-sight connections with ground nodes, rapid deployment, and adjustable mobility [2]. With such attributes, UAVs can serve as aerial base stations (BSs) or relays in conjunction with terrestrial base stations, resulting in aerial-terrestrial integrated networks (ATINs). By connecting cell-edge user devices (UDs) to terrestrial cellular networks via aerial BSs or relays, ATINs improve coverage and connectivity significantly [3]. The 3GPP standard incorporates using UAVs as a communication infrastructure to complement terrestrial cellular networks as well [4]. During current 5G deployment efforts, it has been shown that the millimeter-wave band at 28 GHz has a significantly larger bandwidth than the sub-6 GHz band. At the same time, air-to-ground communications can avoid blockages and maintain LOS connectivity due to UAV's high altitude and flexibility [5]. Therefore, the mmWave band is suitable for deploying high-capacity ATINs in next-generation cellular networks.

A data-driven decision-making process enables wireless networks to manage radio resources more efficiently by predicting and analyzing several dynamic factors, such as users' behavior, mobility patterns, traffic congestion, and quality-of-service expectations. Data-driven radio resource management (RRM) has gained increasing popularity thanks to the expansion of wireless sensing applications, enormous data availability, and devices' increasing computing capabilities. To train machine learning (ML) models, raw data collected from individual UDs is aggregated in a central parameter server (CPS). As a result, such centralized ML approaches require enormous amounts of network resources to collect raw data from UDs. In addition, centralized ML also impairs users' privacy since CPS can easily extract sensitive information from raw data gathered from UDs. Recently, Google proposed federated learning (FL) for UDs to collaboratively learn a model without sharing their private data [6]. In FL, UDs update parameters according to their local datasets; only the most recent parameters are shared with the CPS. Using local models from all participating UDs, the CPS updates global model parameters and shares them with the UDs. The local and global models are adjusted iteratively until convergence. Unlike centralized ML approaches, FL protects UDs' privacy and improves wireless resource utilization significantly. Nevertheless, the convergence performance of FL in wireless networks significantly depends on the appropriate selection of the participating UDs, based on channel and data quality, and bandwidth allocation among the selected UDs [7].

Recently, UAV-supported FL has emerged as an integral component for decentralized decision-making in the ATINs of beyond the 5G era [8]. UAV-supported FL frameworks can leverage UAVs in two different ways. In particular, UAVs are frequently used as aerial sensors, where UAVs collect data using their on-board sensors (e.g., camera and air quality meter) and participate in FL by training models locally and sharing model parameters with the CPS [9]. Meanwhile, 6G ATINs can also deploy UAVs with edge computing capabilities, denoted onboard radio access node (UxNB), to extend the coverage or increase the cellular capacity by acting as an aerial BS or aerial relay [10]. In this context, UAV (i.e., UxNB) can be leveraged in building the FL model as a global model aggregator for a large number of ground UDs, thanks to its large coverage and high probability of establishing LOS communications [11]. However, in both use cases of the UAV-supported FL framework, the convergence and accuracy of FL notably depend on appropriately exploiting the unique attributes of air-to-ground communication links.

This work focuses on the UAV-assisted FL framework, where a swarm of UAVs are deployed in an mmWave ATIN to provide global model aggregation capability to the ground UDs. Conventionally star-based FL is exploited for such UAV-supported FL framework, where all the local model parameters are aggregated from UDs to a single UAV (i.e., CPS) using the air-to-ground communication links. Although such a star-based FL is convenient, it poses several challenges in the context of mmWave ATINs. First, a star-based FL requires a longer convergence time due to the presence of straggling local learners. Recall the duration of transmission and hovering of a UAV influences its energy consumption, and consequently, the increased convergence time of FL directly increases the energy consumption of UAVs. This presents a significant challenge for implementing UAV-supported FL in ATINs since UAVs usually have limited battery capacity. In addition, due to the increased distance and other channel impairments, a number of local learners (i.e., ground UDs) with excellent datasets may fail to establish reliable links with the UAV-mounted global aggregator and are excluded from building the FL model. This can notably affect the overall accuracy of the developed FL model. The use of star-based FL frameworks in mmWave ATINs is also confronted by the uncertainty of air-to-ground communication links resulting from random blocking and the mobility of UAVs. To address these challenges and fully exploit the capability of UAV swarms, a distributed FL scheme is required. This work aims to achieve this goal by proposing a resource-efficient FL framework for mmWave ATINs that incorporates decentralized model dissemination and energy-efficient UD scheduling to UAVs while leveraging both UAV-to-UAV and UD-to-UD collaborations.

A. SUMMARY OF THE RELATED WORKS

In the current literature, communication-efficient FL design problems are explored. In [12], the authors suggested a stochastic alternating direction multiplier method to update the local model parameters while reducing communications between local learners and CPS. In [13], a joint client scheduling and RRB allocation scheme was developed to minimize accuracy loss. To minimize the loss function of FL training, UD selection, RRB scheduling, and transmit power allocation were optimized simultaneously [14]. The number of global iterations and duration of each global iteration were minimized by jointly optimizing the UD selection and RRB allocation [15]. Besides, since UDs participating in FL are energy-constrained, many studies have focused on designing energy-efficient FL frameworks. As demonstrated in [16], the energy consumption of FL can be reduced by uploading only quantized or compressed model parameters from UDs to CPS. Furthermore, RRM enhances the energy efficiency of FL in large-scale networks. Several aspects of RRM, such as client scheduling, RRB allocation, and transmit power control, were extensively studied to minimize both communication and computation energy of FL frameworks [17], [18]. An energy-efficient FL framework based on relay-assisted two-hop transmission and a non-orthogonal multiple access scheme was recently proposed for energy and resource-constrained Internet of Things (IoT) networks [19]. In the aforesaid studies, conventional star-based FL frameworks were studied. Due to its requirement to aggregate all local model parameters on a single server, the star-based FL is inefficient for energy- and resource-constrained wireless networks.

Hierarchical FL (HFL) frameworks involve network edge devices uploading model parameters to mobile edge computing (MEC) servers for local aggregation, where the MEC servers upload aggregated local model parameters to CPS periodically. The HFL framework increases the number of connected UDs and reduces energy consumption [20]. To facilitate the HFL framework, a client-edge-cloud collaboration framework was explored [21]. HFL was investigated in heterogeneous wireless networks by introducing fog access points and multiple-layer model aggregation [22]. Dynamic wireless channels in the UD-to-MEC and MEC-to-CPS hops and data distribution are crucial in FL learning accuracy and convergence. Thus, efficient RRM is imperative for the implementation of HFL. As a result, existing literature evaluated several RRM tasks, including UD association, RRB allocation, and edge association, to reduce cost, latency, and learning error of HFL schemes [23], [24].

While HFL increases the number of participating UDs, its latency and energy consumption are still hindered by dual-hop communication for uploading and broadcasting local and global model parameters. Server-less FL is a promising alternative to reduce latency and energy consumption. This FL framework allows UDs to communicate locally aggregated models without involving central servers, thereby achieving model consensus. The authors in [25] proposed an FL scheme that relies on device-to-device (D2D) communications to achieve model consensus. However, this FL scheme has limited latency improvement due to the requirement of global model aggregation with two-time scale FL over both D2D and user-to-CPS wireless transmission. In [26] and [27], the authors developed FL model dissemination schemes by leveraging connected edge servers (ESs), which aggregate local models from their UD clusters and exchange them with all the other ESs in the network for global aggregation. However, a fully connected ES network is prohibitively expensive in practice, especially when ESs are connected by wireless links. In addition, each global iteration of the FL framework takes significantly longer because ESs continue to transmit local aggregated models until all other ESs receive them successfully [26], [27]. In [28], we addressed this issue by introducing conflicting UDs, which are the UDs residing in the overlapping zones of neighboring clusters, and allowing parameter exchanges among such conflicting UDs and local model aggregators.

In spite of recent advances in resource-efficient, hierarchical, and decentralized FL frameworks, existing studies have several limitations in utilizing UAVs as local model aggregators in mmWave ATINs. In particular, state-of-the-art HFL schemes of [21], [22], and [23] can prohibitively increase UAVs' communication and propulsion energy consumption because they involve two-hop communications and increased latency. Although energy-efficient FL frameworks were considered in our prior studies [19], such study considered conventional HFL framework and did not consider the notion of decentralized model dissemination. Additionally, the mmWave band requires LOS links between UDs and UAVs for local model aggregation and LOS UAV-to-UAV links for model dissemination. Accordingly, the FL model dissemination frameworks proposed in [26], [27], and [28] will not be applicable to mmWave ATINs. Many research studies have highlighted the importance of UAVs in enhancing various performance metrics. For instance, UAVs can help in reducing the total network energy consumption, minimizing the average age of information, and meeting the strict latency requirements of less than 100 milliseconds for supporting real-time applications of mobile edge systems [29]. Moreover, UAVs can improve system resources through device-to-device (D2D) communication [30] and enhance learning accuracy in UAV-assisted HFL systems [31]. We emphasize that in order to maintain convergence speed and reduce energy consumption, the interaction among UD-to-UAV associations, RRB scheduling, and UAV-to-UAV link selection, in addition to the inherent properties of mmWave bands, must be appropriately characterized. This fact motivates us to develop computationally efficient model dissemination and RRM schemes for mmWave ATINs implementing decentralized FL.

B. CONTRIBUTIONS

The key motivation of deploying UAVs as the local model aggregators is that the flexible deployment of UAV allows to establish short-distance LOS communications over the mmWave band to the geographically distant UDs, enabling a large number of UDs to participate in FL and reducing the probability of occurrence of straggling UDs [16], [17]. Furthermore, thanks to higher transmit power than UDs and favorable LOS communications, UAVs can rapidly exchange locally aggregated parameters with each other. Specifically, a single UAV cannot provide LOS coverage to many geographically distributed UDs (i.e., data owners). Accordingly, we deploy multiple UAVs to provide LOS coverage to as many UDs as possible and enable collaboration among these UAVs to achieve rapid convergence of FL while using LOS UAV-to-UAV links. Our proposed UAV-based solution is also advantageous for conducting FL in rural wireless networks and battlefields without centralized infrastructure.

In this work, we investigate the problem of developing an efficient FL model for ATINs, where a swarm of UAVs with edge computing capabilities are deployed to collect and aggregate model parameters from many distributed ground UDs over mmWave channels. The considered UAV-assisted FL is particularly efficient in remote or out-of-network coverage areas such as battlefields, forests, and disaster-affected zones, where centralized infrastructure (such as BS) is either absent or malfunctioned for global model aggregation. To efficiently exploit UAV swarm for conducting FL in mmWave ATINs, this work proposes a resource-efficient and fast-convergent FL framework, referred to as Federated Learning with Model Dissemination (FedMoD), with two distinct features.

- **UAV-enabled Model Dissemination:** FedMoD enables decentralized model parameter dissemination by utilizing UAVs as local model aggregators and taking advantage of UAV-to-UAV and D2D communications. With the potential to place UAVs near cell edge UDs, the proposed UAV-based model parameter collection and aggregation significantly increases the number of participating UDs in the FL model construction process.
- **Enhanced Energy Efficiency:** FedMoD also ensures energy-efficient model training subject to certain FL latency constraints, making it particularly suitable for UAV-enabled FL in ATINs. Unlike the conventional centralized FL schemes, FedMoD effectively exploits collaborations among the UAVs to build both resource-efficient and energy-efficient FL models.

To the best of the authors' knowledge, this is the first work that develops a decentralized FL framework specifically tailored for mmWave ATINs while considering the characteristics of the communication channels. The specific contributions of this work are summarized as follows.

- A UAV-based distributed FL model aggregation method is proposed by leveraging UAV-to-UAV communications. Through the proposed method, each UAV is able to collect local model parameters only from the UDs in its coverage area and share those parameters over LOS mmWave links with its neighbor UAVs. The notion of physical layer network coding is primarily used for disseminating model parameters among UAVs. This allows each UAV to collect all of the model parameters and aggregate them globally without the involvement of the CPS. Based on the channel capacity of the UAV-to-UAV links, a conflict graph is established to facilitate the distributed model dissemination among the UAVs and a maximal weighted independent search (MWIS) method is proposed to solve the conflict graph problem. A decentralized FL algorithm is developed in light of the derived solutions, and its convergence is rigorously proved.
- Additionally, a novel RRM scheme is investigated to reduce the overall energy consumption of the developed decentralized FL framework under the constraint of learning latency. The proposed RRM optimizes both (i) the scheduling of LOS UDs to suitable UAVs and radio resource blocks (RRBs) over mmWave links and (ii) the scheduling of non-LOS UDs to LOS UDs over side-link D2D communications such that non-LOS can transmit their model parameters to UAVs with the help of available LOS UDs. Both scheduling problems are provably NP-hard, so their optimal solutions require prohibitively complex computational resources. Therefore, two graph theory solutions are proposed for the aforementioned scheduling problems to strike a suitable balance between optimality and computational complexity.
- To verify FedMoD's effectiveness over contemporary star-based FL and HFL schemes, extensive numerical simulations are conducted. Simulation results reveal that FedMoD achieves good convergence rates and superior energy consumption compared to the benchmark schemes.

The rest of this paper is organized as follows. In Section II, the system model is described in detail. In Section III, the proposed FedMoD algorithm is explained thoroughly along with its convergence analysis. Section IV presents the energy consumption problem elements of the decentralized FL. Section V presents the RRM scheme for improving the energy efficiency of the proposed FedMoD framework. Section VI presents various simulation results on the performance of the proposed FedMoD scheme. Finally, the concluding remarks are provided in Section VII.

II. SYSTEM MODEL

A. SYSTEM OVERVIEW

The envisioned mmWave ATIN model is illustrated in Fig. 1, which consists of a single CPS, a swarm of UAVs with edge computing capability that can talk to each other through mmWave air-to-air (A2A) links, and multiple ground UDs that are under the serving region of each UAV. The UDs are connected with the UAVs via mmWave ground-to-air (G2A) links. In this system model, UDs own the local datasets and train models locally, whereas UAVs collect and aggregate the locally trained model parameters. In particular, we assume that UDs are far from the CPS and cannot directly transmit the locally trained model parameters to CPS. Hence, we leverage UAV swarm for global model aggregation. Notably, each UAV can collect local parameters from only a set of UDs with LOS mmWave connections. To this end, we develop a decentralized model dissemination framework while exploiting UAV-to-UAV and D2D communications to build the global FL model. Although we entirely offload the CPS to perform global aggregation, the CPS is still required to coordinate the clustering optimization of UAVs and their associated UDs through reliable control channels.

The set of all the considered UDs is denoted by $\mathcal{U} = \{1, 2, \cdots, U\}$ and the set of UAVs is denoted by $\mathcal{K} = \{1, 2, \cdots, K\}$. The FL process is organized in iterations, indexed by $\mathcal{T} = \{1, 2, \cdots, T\}$. Similar to the resource settings in [32] and [33], each UAV k is granted a limited number of B_k orthogonal RRBs, and the total number of granted RRBs for all the UAVs is denoted by the set $\mathcal{B} = \{1, 2, \cdots, B\}$. The UDs are scheduled to these RRBs to offload their local parameters to the UAVs. The set of UDs in the serving region of the k-th UAV is denoted by $\mathcal{U}_k = \{1, 2, \cdots, U_k\}$. In addition, for the u-th UD, the set of available UAVs with LOS connectivity is denoted by a

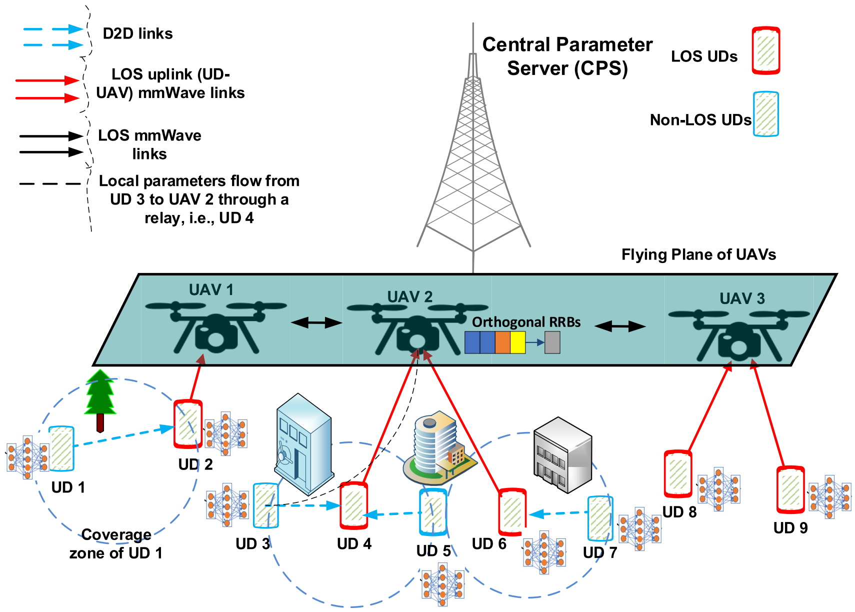

FIGURE 1. **A typical ATIN network with one CPS, 3 UAVs, 9 UDs, and a set of RRBs per each UAV.**

set $\mathcal{K}_u$. For the analytical tractability, we make the following assumptions. **A1:** In a given FL iteration, each ground UD is associated with only one UAV over LOS mmWave G2A links. However, different FL iterations can change the association between a UAV and a UD. **A2:** The UDs transmit their locally trained model parameters to the associated UAV over orthogonal RRBs as such there is no co-channel interference among the concurrently scheduled UDs to a given UAV. We also assume that D2D communications also exploit orthogonal RRBs and therefore, we do not consider interference among the concurrently scheduled D2D links. **A3:** Each UAV broadcasts the aggregated global model parameters to its scheduled UDs over orthogonal RRBs as such all the UDs can decode the received models.

The assumption **A1** is considered since, due to the directional RF signal propagation characteristics of the mmWave band, a ground UD can only be associated with a single UAV as long as it has a clear LOS path. However, the association between a UAV and a UD is changed in different FL iterations due to the inherent mobility of UDs and UAVs. Meanwhile, assumptions **A2** and **A3** are considered to avoid interference in model parameter transmission and reception phases. Note that assumptions **A2** and **A3** are also considered with the existing cellular communication standards, where orthogonal frequency division multiple access (OFDMA) is adopted to avoid interference among the simultaneously transmitting/receiving UDs.

B. COMMUNICATION MODEL

Suppose that the k-th UAV flies, and hovers at a fixed flying altitude H_k, and all the UAVs are assumed to have the same altitude. Let $\mathbf{x}_l = (x_k, y_k, H_k)$ is the 3D location of the k-th UAV and (x_u, y_u) is the 2D location of the u-th UD. In accordance with [34], for the mmWave UD-UAV communications to be successful, one needs to ensure LOS connectivity between UAVs and UDs. However, some of the UDs may not have LOS communications to the UAVs, thus they can not transmit their trained local parameters directly to the UAVs. Let $\mathcal{U}_{los}$ be the set of UDs that have LOS links to the UAVs, and let $\mathcal{U}_{non}$ be the set of UDs that do not have LOS links to the UAVs. Given an access link between the u-th UD, i.e., $u \in \mathcal{U}_{los}$, and the k-th UAV, the path loss of the channel (in dB) between the u-th UD and the k-th UAV is expressed as follows $PL(u,k) = 20\log_{10}(\frac{4\pi f_c d_{u,k}}{c})$, where f_c is the carrier frequency, and c is the light speed, and $d_{u,k}$ is the distance between the u-th UD and the k-th UAV [34]. The wireless channel gain between the u-th UD and the k-th UAV on the b-th RRB is $h^u_{k,b} = 10^{-PL(u,k)/10}$. Let p be the transmission power of the UDs and maintains fixed and N_o as the AWGN noise power. Therefore, the achievable capacity at which the u-th UD can transmit its local model parameter to the k-th UAV on the b-th RRB at the t-th global iteration is given by Shannon's formula $R^u_{k,b} = W\log_2(1 + \frac{p|h^u_{k,b}|^2}{N_0}), \forall u \in \mathcal{U}_k, k \in \mathcal{K}_u$, where $\mathcal{U}_k \subset \mathcal{U}_{los}$ and W is the RRB's bandwidth. Note that the transmission rate between the u-th UD and the k-th UAV on the b-th RRB determines if the k-th corresponding UAV covers the u-th UD and has LOS to the u-th UD. In other words, the u-th UD is within the coverage of the k-th corresponding UAV if $R^u_{k,b}$ meets the rate threshold R_0, i.e., $R^u_{k,b} \geq R_0$, and has LOS link to the k-th UAV. Each UAV k, $\forall k \in \mathcal{K}$ aggregates the local models of its scheduled UDs only.

To disseminate the local aggregated models among the UAVs to reach global model consensus, each UAV communicates with its neighbor UAVs through mmWave A2A links. To guarantee global convergence, each UAV must receive the locally aggregated model parameters from all other UAVs in the network. To this end, we exploit Algorithm 1 of Section III-B to find suitable neighbors for each UAV as such, the global convergence is accelerated. We consider that LOS A2A links are available among the neighboring UAVs [35]. We also assume that the UAVs employ directive beamforming to improve the transmission rate. The gain of the UAV antenna located at x_k, denoted by G^A, at the receiving UAV is given by [36]

$$G^A(d_{A,x_k}) = \begin{cases} G_m^A, & \text{if } -\dfrac{\theta_b^a}{2} \le \Phi \le \dfrac{\theta_b^a}{2} \\ G_s^A, & \text{otherwise}, \end{cases} \tag{1}$$

where d_{A,x_k} is the distance between the typical receiving UAV and the k-th UAV at x_k, G_m^A, G_s^A are the gains of the main-lobe and side-lobe, respectively, and Φ is the sector angle, $\theta_b^a \in [0, 180]$ is the beamwidth in degrees [37]. Accordingly, the received power at the typical receiving UAV from UAV k at x_k is given by

$$P_{r,k}^A = PG^A(d_{A,x_k})\zeta_A H_A^{x_k} d_{A,x_k}^{-\alpha_A}, \tag{2}$$

where ζ_A represents the excess losses, $H_A^{x_k}$ is the Gamma-distributed channel power gain, i.e., $H_A^{x_k} \sim \Gamma(m_A, \frac{1}{m_A})$, with a fading parameter m_A, α_A is the path-loss exponent, and P is the transmit power of UAVs and maintains fixed. As a result, the SINR at the typical receiving UAV is given by

$$\gamma = \frac{\mu_A H_A^{x_k} d_{A,x_k}^{-\alpha_A}}{I + \sigma^2}, \tag{3}$$

where $\mu_A = P_A G_m^A \zeta_A$, I is the interference power. Such interference can be expressed as follows

$$I = \sum_{j=1, j\neq k}^{K} PG^A(d_{A,x_j})\zeta_A H_A^{x_j} d_{A,x_j}^{-\alpha_A}, \tag{4}$$

where $G^A(d_{A,x_j}) = G_m^A$ with a probability of q_A and $G^A(d_{A,x_j}) = G_s^A$ with a probability of $1 - q_A$.

Once the local aggregated model dissemination among the UAVs is completed, the k-th UAV adopts a common transmission rate R_k that is equal to the minimum achievable rates of all its scheduled UDs $\mathcal{U}_k$. This adopted transmission rate is $R_k = \min_{u\in\mathcal{U}_k} R_u^k$, which is used to transmit the global model to the UDs to start the next global iteration.

C. TRANSMISSION TIME STRUCTURE

The UAVs start local model aggregations after receiving the locally trained models of the scheduled UDs across all the RRBs. Since different UDs $\mathcal{U}_{los}$ will have different transmission rates, they will have different transmission durations for uploading their trained parameters to the UAVs/RRBs. Let s be the size of the UD's local vector parameter (which is the same for the global model), expressed in bits. Note that the analysis in this subsection is for the transmission duration of one global iteration t. For simplicity, we represent X as the number of elements in the set $\mathcal{X}$. The time required by the u-th UD, $u \in \mathcal{U}_{los}$, to reliably transmit its model update to the k-th selected UAV over the b-th RRB is then given by $T_u^{com} = \frac{s}{R_{k,b}^u}$. With this consideration, we can see that, given the number of participating UDs U_{los}, the transmission duration is $T_u = \max_{u\in\mathcal{U}_{los}}\{T_u^{com}\} = \max_{u\in\mathcal{U}_{los}} \frac{s}{R_{k,b}^u}$. When U_{los} is large, $\max_{u\in\mathcal{U}_{los}}\{T_u^{com}\}$ can dramatically grow. The minimum rate of the scheduled UDs is expressed by $R_{min}^u = \min_{u\in\mathcal{U}_{los}}\{R_{k,b}^u\} = \min_{u\in\mathcal{U}_{los}} W \log_2(1 + \frac{p|h_{k,b}^u|^2}{N_0})$. The transmission duration is therefore constrained by this minimum rate. Without the loss of generality, let us assume that UD $u \in \mathcal{U}_{los}$ has the minimum rate R_{min}^u. The corresponding transmission duration is $\frac{s}{R_{min}^u}$. The selection of R_{min}^u dominates the local model's transmission duration from the UDs to the UAVs, thus, it dominates the time duration of one FL global iteration. This is because the FL time consists of the local model transmission time and the learning computation time. Since the computation times of the UDs for local learning do not differ much, the FL time of one global iteration is dominated by R_{min}^u. Thus, R_{min}^u can be adapted to include fewer or more UDs in the training process.

For the different transmission durations $\mathcal{U}_{los}$, some UDs will finish transmitting their local models before other UDs. Thus, high transmission rate UDs in $\mathcal{U}_{los}$ will have to wait to start a new iteration simultaneously with relatively good transmission rate UDs. We propose efficiently exploiting such waiting times to assist the UDs with non-LOS channels to the UAVs. Define the portion of the time that not being used by $\bar{u}$-th UD (i.e., $\bar{u} \neq u, u \in \mathcal{U}_{los}$) at the t-th iteration is referred to as the idle time of the $\bar{u}$-th UD and denoted by $T_{idle}^{\bar{u}}$. This idle time can be expressed as $T_{idle}^{\bar{u}} = (\frac{s}{R_{k,b}^{\bar{u}}} - \frac{s}{R_{min}^u})$ seconds. Such idle time can be exploited by UDs $\bar{u} \in \mathcal{U}_{los}$ via D2D links if they ensure the complete transmission of the local parameters of the non-LOS UDs to the UAVs. More specifically, the idle time of the $\bar{u}$-th UD should be greater than or equal to the transmission duration of sending the local parameters from the $\hat{u}$-th non-LOS UD to the $\bar{u}$-th UD plus the time duration of forwarding the local parameters from the $\bar{u}$-th UD to the k-th UAV. Mathematically, it must satisfy $T_{idle}^{\bar{u}} \geq (\frac{s}{R_{\hat{u}}^{\bar{u}}} + \frac{s}{R_{k,b}^{\bar{u}}})$. From now on, we will use the term relay to UD $\bar{u} \neq u, \bar{u} \in \mathcal{U}_{los}$. In relay mode, each communication period is divided into two intervals corresponding to the non-LOS UD-relay phase (D2D communications) and the relay-UAV phase (mmWave communication). The aforementioned transmission duration components of UDs and relays for one global iteration are shown in Fig. 2. Note that UDs can re-use the same frequency band and transmit simultaneously via D2D links.

When the $\hat{u}$-th UD does not have a LOS communication to any of the UAVs, it may choose the $\bar{u}$-th UD as its relay if the $\bar{u}$-th relay is located in the coverage zone of the $\hat{u}$-th UD. Let $\mathcal{U}_{\hat{u}}$ be the set of relays in the coverage zone of UD $\hat{u}$. Let $h_{\hat{u}}^{\bar{u}}$ denote the channel gain for the D2D link between the $\hat{u}$-th UD

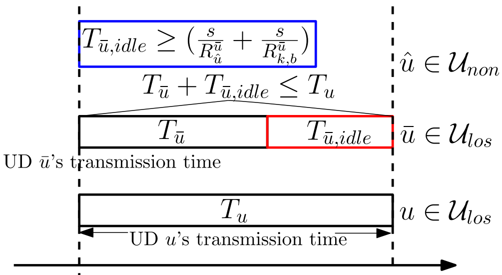

FIGURE 2. Transmission time structure for LOS UDs and non-LOS UDs for the t-th global iteration.

and the $\bar{u}$-th relay. Then, the achievable rate of D2D pair $(\hat{u}, \bar{u})$ is given by $R^{\bar{u}}_{\hat{u}} = W \log_2(1 + \frac{p|h^{\bar{u}}_{\hat{u}}|^2}{N_0}), \forall \bar{u} \in \mathcal{U}_{los}, \hat{u} \in \mathcal{U}_{non}$. In relay mode, the transmission duration for sending the local parameter of the $\hat{u}$-th UD to the k-th UAV through relay $\bar{u}$ is $\mathtt{T}_{\hat{u}} = \frac{s}{R^{\bar{u}}_{\hat{u}}} + \frac{s}{R^{\bar{u}}_{k,b}}$, which should satisfy $\mathtt{T}_{\hat{u}} \leq T^{\bar{u}}_{idle}$.

Remark 1: Similar to [2], [9], [11], and [28] we consider that UAVs remain static at each global FL iteration and they collect model parameters from their LOS UDs, locally aggregate them, exchange such locally aggregated parameters with the neighbor UAVs for global aggregation, and send the globally aggregated parameters to ground UDs. Such a consideration has two reasons. First, a single global iteration requires a fraction of a second time to ensure fast convergence of FL. Meanwhile, moving UAVs from one location to another location requires time in the order of seconds [38]. Second, if UAVs remain mobile within a global FL iteration, their neighbor UAVs and UAV-to-UAV communication channels would rapidly change, causing instability to the proposed model dissemination and decentralized FL framework. It is noteworthy that UAVs change their positions using a predefined trajectory at the end of each global FL iteration, and can be associated with new UDs. This allows UAVs to collect local FL parameters from a large set of geographically distant UDs by providing them LOS connectivity over mmWave channels. However, the joint optimization of UAVs' trajectories and resource scheduling to optimize FL performance is beyond the scope of the current work, and will be considered in the future extension of this paper.

Remark 2: We propose a novel synchronous FL, where we efficiently exploit the waiting times to assist the UDs that have non-LOS channels to the UAVs. Such FL framework results in more accommodated UDs than its synchronous counterparts (i.e., HFL and star-based FL).

III. FedMoD: DEVELOPMENT OF DECENTRALIZED FL FRAMEWORK

A. FEDERATED LEARNING PROCESS

Each UD u in FL possesses a set of local training data, denoted as $\mathcal{D}_u$. The local loss function on the dataset of the u-th UD can be calculated as

$$F_u(\mathbf{w}) = \frac{1}{|\mathcal{D}_u|} \sum_{(x_i,y_i)\in\mathcal{D}_u} f_i(\mathbf{w}), \forall u \in \mathcal{U}, \tag{5}$$

where x_i is the sample i's input (e.g., image pixels) and y_i is the sample i's output (e.g., label of the image) and $f_i(\mathbf{w})$ is the loss function that measures the local training model error of the i-th data sample. The collection of data samples at the set of UDs that is associated with the k-th UAV is denoted as $\tilde{\mathcal{D}}_k$, and the training data at all the learning involved UDs, denoted as $\mathcal{U}_{inv}$, is denoted as $\mathcal{D}$. The ratios of data samples are defined as $\hat{m}_u = \frac{|\mathcal{D}_u|}{|\tilde{\mathcal{D}}_k|}$, $m_u = \frac{|\mathcal{D}_u|}{|\mathcal{D}|}$, and $\tilde{m}_k = \frac{|\tilde{\mathcal{D}}_k|}{|\mathcal{D}|}$, respectively. We define the loss function for the k-th UAV as the average local loss across the k-th cluster $\hat{F}(\mathbf{w}) = \sum_{u=1}^{|\mathcal{U}_k|} \frac{|\mathcal{D}_u|}{|\tilde{\mathcal{D}}_k|} F_u(\mathbf{w})$. The global loss function $F(\mathbf{w})$ is then defined as the average loss across all the clusters $F(\mathbf{w}) = \sum_{u=1}^{|\mathcal{U}_{inv}|} \frac{|\mathcal{D}_u|}{|\mathcal{D}|} F_u(\mathbf{w})$. The objective of the FL model training is to find the optimal model parameters $\mathbf{w}^*$ for $F(\mathbf{w})$ that is expressed as follows $\mathbf{w}^* = \arg\min_{\mathbf{w}} F(\mathbf{w})$. In this work, we propose FedMoD that involves three main procedures: 1) local model update at the UDs, 2) local model aggregation at the UAVs, and 3) model dissemination between the UAVs.

1) LOCAL MODEL UPDATE

Denote the model of the u-th UD at the t-th global iteration as $\mathbf{w}_u(t)$. This UD performs model updating based on its local dataset by exploiting the stochastic gradient descent (SGD) algorithm, expressed as

$$\mathbf{w}_u(t) = \mathbf{w}_u(t-1) - \lambda g(\mathbf{w}_u(t-1)), \tag{6}$$

where λ is the learning rate and $g(\mathbf{w}_u(t-1))$ is the stochastic gradient computed on the dataset of the u-th UD.

2) LOCAL MODEL AGGREGATION

After all the selected UDs complete their local model updates, they offload their model parameters over the available RRBs to the associated UAVs. A typical UAV k aggregates the received models by computing a weighted sum as follows

$$\tilde{\mathbf{w}}_k(t) = \sum_{u\in\mathcal{U}_k} \hat{m}_u \mathbf{w}_u(t), \forall k \in \mathcal{K}. \tag{7}$$

3) MODEL DISSEMINATION

Each UAV disseminates its local aggregated model to the one-hop neighboring UAVs. The model dissemination includes $l = 1, 2, \cdots, \alpha$ times of model dissemination until at least one UAV receives the local aggregated models of other UAVs, where α is the number of dissemination rounds. Specifically, at the t-th iteration, the k-th UAV aggregates the local models of its associated UDs as in (7).

At the beginning of the model dissemination step, the k-th UAV knows only $\tilde{\mathbf{w}}_k(t)$ and does not know the models of other UAVs' models $\tilde{\mathbf{w}}_j(t), j \neq k, \forall j \in \mathcal{K}$. Consequently, at the t-th global iteration and l-th round, the k-th UAV has the following two sets:

- The *Known* local aggregated model: Represented by $\mathcal{H}^l_k(t) = \{\tilde{\mathbf{w}}_k(t)\}$.
- The *Unknown* local aggregated models: Represented by $\mathcal{W}^l_k(t) = \{\tilde{\mathbf{w}}_j(t), \tilde{\mathbf{w}}_{\bar{j}}(t), \cdots, \tilde{\mathbf{w}}_K(t)\}$ and defined as the set of the local aggregated models of other UAVs.

These two sets are referred as the side information of the UAVs. For instance, at $l = \alpha$, the side information of the k-th UAV is $\mathcal{H}_k^{\alpha}(t) = \{\tilde{\mathbf{w}}_k(t), \tilde{\mathbf{w}}_j(t), \tilde{\mathbf{w}}_{\bar{j}}(t), \cdots, \tilde{\mathbf{w}}_K(t)\}$ and $\mathcal{W}_k^{\alpha}(t) = \emptyset$. To achieve global model consensus, UAV k needs to know the other UAVs' models, i.e., $\mathcal{W}_k(t)$, so as to aggregate a global model for the whole network. To this end, we propose an efficient model dissemination scheme, detailed in Section III-B, enabling the UAVs to obtain their *Unknown* local aggregated models $\mathcal{W}_k(t), \forall k \in \mathcal{K}$, with minimum dissemination latency.

B. MODEL DISSEMINATION

This section develops a distributed model dissemination scheme that overcomes the need for CPS for global aggregations or UAV coordination. Note that all the associations of UAVs $\mathcal{K}_k$ can be computed locally at the k-th UAV since all the needed information (e.g., complex channel gains and the indices of the local aggregated models) are locally available. In particular, UAV $k \in \mathcal{K}$ knows the information of its neighboring UAVs only.

At each dissemination round, transmitting UAVs use the previously mentioned side information to perform XOR model encoding, while receiving UAVs need the stored models to obtain the *Unknown* ones. The entire process of receiving the *Unknown* models takes a short time. According to the reception status feedback by each UAV, the UAVs distributively select the transmitting UAVs and their models to be transmitted to the receiving UAVs at the l-th round, $\forall l$. The transmitted models can be one of the following two options for the i-th receiving UAV, $\forall i$.

- Non-innovative model (NIM): A coded model is non-innovative for the i-th receiving UAV if it does not contain any model that is not known to UAV i.
- Decodable model (DM): A coded model is decodable for the i-th receiving UAV if it contains just one model that is not known to the i-th UAV.

In order to represent the XOR coding opportunities among the models not known at each UAV, we introduce a FedMoD conflict graph. At the l-th round, the FedMoD conflict graph is denoted by $\mathcal{G}(\mathcal{V}(l), \mathcal{E}(l))$, where $\mathcal{V}(l)$ refers to the set of vertices, $\mathcal{E}(l)$ refers to the set of encoding edges. Let $\mathcal{K}_k$ be the set of neighboring UAVs to the k-th UAV, and let $\mathcal{K}_w \subset \mathcal{K}$ be the set of UAVs that still wants some local aggregated models. Hence, the FedMoD graph is designed by generating all vertices for the k-th possible UAV transmitter that can provide some models to other UAVs, $\forall k \in \mathcal{K}$. The vertex set $\mathcal{V}(l)$ of the entire graph is the union of vertices of all possible transmitting UAVs. Consider, for now, generating the vertices of the k-th UAV. Note that the k-th UAV can exploit its previously received models $\mathcal{H}_k^l(t)$ to transmit an encoded/uncoded model to the set of requesting UAVs. Therefore, each vertex is generated for each model $m \in \mathcal{W}_i^l(t) \cap \mathcal{H}_k^l(t)$ that is requested by each UAV $i \in \mathcal{K}_w \cap \mathcal{K}_k$ and for each achievable rate of the k-th UAV $r \in \mathcal{R}_{k,i} = \{r \in \mathcal{R}_k | r \leq r_{k,i} \text{ and } i \in \mathcal{K}_w \cap \mathcal{K}_k\}$, where $\mathcal{R}_{k,i}$ is a set of achievable capacities between the k-th UAV and the i-th UAV, i.e., $\mathcal{R}_{k,i} \subset \mathcal{R}_k$. Accordingly, the i-th neighboring UAV in $\mathcal{K}_k$ can receive a model from the k-th UAV. Therefore, we generate $|\mathcal{R}_{k,i}|$ vertices for a requesting model $m \in \mathcal{H}_k^l(t) \cap \mathcal{W}_i^l(t), \forall i \in \mathcal{K}_w \cap \mathcal{K}_k$. A vertex $v_{i,m,r}^k \in \mathcal{V}(l)$ indicates the k-th UAV can transmit the m-th model to the i-th UAV with a rate r. We define the utility of vertex $v_{i,m,r}^k$ as

$$w(v_{i,m,r}^k) = rN_k, \tag{8}$$

where N_k is the number of neighboring UAVs that can be served by the k-th UAV. This weight metric shows two potential benefits (i) N_k represents that the k-th transmitting UAV is connected to many other UAVs that are requesting models in $\mathcal{H}_k^t(l)$; and (ii) r provides a balance between the transmission rate and the number of scheduled UAVs.

Since UAVs communicate among themselves, their connectivity can be characterized by an undirected graph with sets of vertices and connections. All possible conflict connections between vertices (conflict edges between circles) in the FedMoD conflict graph are provided as follows. Two vertices $v_{i,m,r}^k$ and $v_{i',m',r'}^{k'}$ are adjacent by a conflict edge in $\mathcal{G}$, if one of the following conflict conditions (CC) is true.

- ***CC1.*** *(encoding conflict edge): $(k = k')$ and $(m \neq m')$ and $(m, m') \notin \mathcal{H}_{k'}^l(t) \times \mathcal{H}_k^l(t)$. A conflict edge between vertices in the same local FedMoD conflict graph is connected as long as their corresponding are not decodable to a set of scheduled UAVs.*
- ***CC2.*** *(rate conflict edge): $(k = k')$ and $(k \neq k')$ and $(r \neq r')$. All adjacent vertices correspond to the same (or different) UAV k and should have the same achievable rate.*
- ***CC3.*** *(transmission conflict edge): $(k \neq k')$ and $(i = i')$. The same UAV cannot be scheduled to two different UAVs k and k'.*
- ***CC4.*** *(half-duplex conflict edge): $(k = i')$ or $(k' = i)$. The same UAV can not transmit and receive in the same dissemination round.*

To distribute the local aggregated models among the UAVs, we propose a graph theory method as follows. Let $\mathcal{S}_k$ represent the associations of the neighboring UAVs in the coverage zone of the k-th UAV, i.e., the associations of UAV k to the set $\mathcal{K}_k$. Then, let the local FedMoD conflict graph $\mathcal{G}_k(\mathcal{S}_k) \subset \mathcal{G}$ for an arbitrary UAV $k \in \mathcal{K}$ represent the set of associations $\mathcal{S}_k$. Our proposed distributed algorithm has two phases: i) the initial phase and ii) the conflict solution phase. In the initial phase, UAV $k \in \mathcal{K}$ constructs the local FedMoD conflict graph $\mathcal{G}_k(\mathcal{S}_k)$ and selects its targeted neighboring UAVs using the maximum weight independent set (MWIS) search method that results in MWIS $\mathbf{S}_k$. Each UAV exchanges its scheduled UAVs with its neighbor UAV. Then, the conflict solution phase starts. The UAV that is associated with multiple UAVs (UAV that is located at the overlapped regions of UAVs) is assigned to one UAV that offers the highest weight of scheduling that UAV. UAVs that do not offer the maximum weight cannot schedule that UAV and therefore, remove that

Algorithm 1 Distributed UAV-UAV Scheduling for Model Dissemination

Data: $\mathcal{K}$, $\tilde{\mathbf{w}}_k$, $\mathcal{H}_k^0(t)$, $\mathcal{W}_k^0(t)$, $\forall k \in \mathcal{K}$.
Initialize Phase:
Initialize: $\mathtt{K} = \emptyset$.
for ***all*** $k \in \mathcal{K}$ **do**
  Construct $\mathcal{G}_k(\mathcal{K}_k)$ and calculate weight $w(v)$ using (8), $\forall v \in \mathcal{G}_k$.
  Find MWIS $\mathbf{S}_k$.
end for
Conflict Solution Phase: **for** $i = 1, 2, \cdots$ **do**
  Transmit $\hat{\mathbf{S}}_k = \{j \in \mathcal{K}_k \mid j \in \mathbf{S}_k\}$.
  Set $\mathtt{K} = \{j \in \mathcal{K} \mid \exists (k, k') \in \mathcal{K}^2, j \in \hat{\mathbf{S}}_k \cap \hat{\mathbf{S}}_{k'}\}$.
  for ***all*** $j \in \mathtt{K}$ **do**
    Set $\hat{\mathcal{K}}(j) = \{k \in \mathcal{K} \mid j \in \hat{\mathbf{S}}_k\}$.
    for ***all*** $k \in \hat{\mathcal{K}}(j)$ **do**
      Set $M_{kj} = \sum_{v\in\mathbf{S}_k} w(v)$ and $\mathcal{K}_k = \mathcal{K}_k \backslash \{j\}$.
      Construct $\mathcal{G}_k(\mathcal{K}_k)$ and compute $w(v)$ by (8) and solve $\tilde{\mathbf{S}}_k$ MWIS.
      Set $\tilde{M}_{kj} = \sum_{v\in\tilde{\mathbf{S}}_k} w(v)$ and transmit M_{kj} and $\tilde{M}_{kj}$.
    end for
    Set $k^* = \arg\max_{k\in\hat{\mathcal{K}}(j)} \left(M_{kj} + \sum_{k'\in\hat{\mathcal{K}}(j), k\neq k'} \tilde{M}_{k'j}\right)$.
    Set $\mathcal{K}_{k^*} = \mathcal{K}_{k^*} \cup \{j\}$.
    for ***all*** $k \in \hat{\mathcal{K}}(j)\backslash\{k^*\}$ **do**
      Set $\mathbf{S}_k = \tilde{\mathbf{S}}_k$.
    end for
  end for
end for
Result: $\mathbf{S} = \mathbf{S}_k, \cdots$

UAV from their set of associated UAVs and vertices. We then design the new graph. We repeat this process until all the conflicting UAVs are scheduled to, at most, a single transmitting UAV. The detailed process of the algorithm for a single dissemination round is presented in Algorithm 1. The computational complexity of Algorithm 1 is $\mathcal{O}(\alpha K^2 K_{\text{ave}}^2)$, where K_{ave} is the average number of connected UAVs to a typical UAV [28]. For further illustration, we explain the dissemination method that is implemented at the UAVs through an example as given in Appendix A.

The steps of FedMoD that include local model update, local aggregation at the UAVs, and model dissemination among the UAVs are summarized in Algorithm 2. In addition, the convergence rate of FedMoD is rigorously proved in Appendix B.

IV. FedMoD: ENERGY-EFFICIENCY ENHANCEMENT OF DECENTRALIZED FL

A. FL TIME AND ENERGY CONSUMPTION

1) FL TIME

The constrained FL time at each global iteration consists of both computation and wireless transmission time which is explained below.

Algorithm 2 FedMoD Algorithm

Data: Number of global iterations T, number of local iterations T_l
Initialize: $t = 1$ and start with the same model for each UD u: $\mathbf{w}_u(t-1)$.
for $t = 1, 2, \cdots, T$ **do**
  for *each UD* $u \in \mathcal{U}_{inv}$ *in parallel* **do**
    Update the local model as $\mathbf{w}_u(t)$ according to (5).
  end for
  for *each UAV* $k \in \mathcal{K}$ *in parallel* **do**
    Receive the most updated model from the UDs in $\mathcal{U}_k$.
    Obtain $\tilde{\mathbf{w}}_k(t)$ by performing local model aggregation according to (7).
    for $l = 1, 2, \cdots, \alpha$ **do**
      UAVs disseminate their models among them as explained in Section III-B and Algorithm 1.
    end for
  end for
  Update $\tilde{\mathbf{w}}_k(t-1) = \tilde{\mathbf{w}}_k(t) = \mathbf{w}(t)$.
  Broadcast $\mathbf{w}(t)$ to the UDs in $\mathcal{U}_k$.
  Update $t = t + 1$.
end for
Result: Final global model $\mathbf{w}$.

The wireless transmission time consists of (1) the uplink transmission time for transmitting the local updates from the UDs to the associated UAVs $\mathcal{K}$. This transmission time is already discussed in Section II-C and represented by T_u. (2) The transmission time for disseminating the local aggregated models among the UAVs. The model dissemination time among all the UAVs is T_{diss}, i.e., for one UAV and one dissemination round, $T_{diss} = \frac{s}{r}$, where r is the adopted transmission rate of that UAV. T_{diss} is generalized in (17) in Appendix A. (3) The downlink transmission time for transmitting the local aggregated models from the UAVs to the scheduled UDs $\mathcal{U}$. The downlink transmission time for UAV k can be expressed $T_k^{do} = \frac{s}{R_k}$. On the other hand, the computation time for local learning at the u-th UD is expressed as $T_u^{comp} = T_l \frac{Q_u D_u}{f_u}$, where T_l is the number of local iterations to reach the local accuracy ϵ_l in the u-th UD, Q_u as the number of CPU cycles to process one data sample, and f_u is the computational frequency of the CPU in the u-th UD (in cycles per second).

By combining the aforementioned components, the FL time τ_k at the k-th UAV can be calculated as

$$\begin{aligned}\tau_k &= \max_{u\in\mathcal{U}_k} T_u^{comp} + \max_{u\in\mathcal{U}_k} T_u^{com} + T_k^{do} \\ &= \max_{u\in\mathcal{U}_k} \left\{T_l \frac{Q_u D_u}{f_u}\right\} + \max_{u\in\mathcal{U}_k} \left\{\frac{s}{R_{k,b}^u}\right\} + \frac{s}{R_k}. \qquad (9)\end{aligned}$$

Therefore, the total FL time for all the global iterations T is $\tau = T(\max_{k\in\mathcal{K}}(\tau_k) + T_{diss})$, which should be no more than the maximum FL time threshold $T_{\max}$. This constraint is expressed as

$$\tau = T\Bigg(\underbrace{\max_{u\in\mathcal{U}}\left\{T_l\frac{Q_u D_u}{f_u}\right\}}_{\text{local learning}} + \underbrace{T_u}_{\text{uplink transmission}} + \underbrace{\max_{k\in\mathcal{K}}\left\{\frac{s}{R_k}\right\}}_{\text{downlink transmission}} + \underbrace{T_{diss}}_{\text{dissemination duration}}\Bigg) \leq T_{\max}. \tag{10}$$

Along the same lines of [18], [19], [23], [28], and [33], in this work, we focus on optimizing single FL global iteration's duration due to the following two reasons. First, we consider a time-constrained FL where the total time of executing the entire FL remains less than a given threshold, T_{max} (e.g., a second). Such constraint can be satisfied by ensuring that the maximum possible duration to complete a single global iteration is less than T_{max}/T, where T is the total number of the global FL iterations to converge the FL. Second, the duration of single FL round depends on the scheduling of the LOS UDs to UAVs/RRBs and non-LOS UDs to available LOS UDs. By scheduling a suitable set of UDs at each single round as the local learners, one can avoid straggler UDs and the resultant long waiting time to start model aggregation at the local model aggregators (i.e., UAVs). Accordingly, optimizing duration of the single round of FL enables to satisfy the given FL time constraint.

2) ENERGY CONSUMPTION

The system's energy is consumed for local model training at the UDs, wireless models transmission, and UAVs' hovering in the air. In what follows, we quantify the energy consumed at UDs and UAVs at each global FL iteration.

a: Energy consumption at UDs

In each global FL iteration, a UD consumes energy for computing local model parameter and for uploading the computed parameters to the associated UAV or LOS UD. Both types of energy consumption are explained as follows.

- *UD's computation energy consumption:* The power consumption of the u-th UD to process a single CPU cycle is $\alpha_c f_u^2$, where α_c is a constant related to the switched capacitance [39], [40]. The energy consumption for local computation at the u-th UD is obtained by $E_u^{comp} = T_l Q_u D_u \alpha_c f_u^2$.
- *UD's communication energy consumption:* For the u-th UD, the energy consumption to transmit the local model parameters to the associated UAVs (or LOS UDs) can be denoted by E_u^{com} and calculated as $E_u^{com} = pT_u^{com}$.

Thus, the overall energy consumption of the u-th UD in one global FL iteration is obtained as $E_u^{comp} + E_u^{com}$, $\forall u$.

b: Energy consumption at UAVs

In each global FL iteration, a UAV consumes energy for its hovering/transition and wireless transmission to support both model dissemination and aggregated model parameter transmission. Both types of energy consumption are explained as follows.

- *UAV's mechanical energy consumption:* UAV's need to remain stationary at the air for the entire duration of each global FL iteration and it can change positions at different global FL iterations. Hence, its propulsion energy consumption consists of both hovering and transition energy consumption. UAV's hovering power is expressed as $p^{hov} = \sqrt{\frac{(mg)^3}{2\pi r_p^2 n_p \rho}}$ [2], where m is UAV's weight, g is the gravitational acceleration of the earth, r_p is propellers' radius, n_p is the number of propellers, and ρ is the air density. In general, these parameters of all the UAVs are the same. The hovering time of UAV(s) should be equal to duration of a single FL iteration such that all the UAVs can collect local model parameters from their associated UDs and perform model dissemination. The duration of a single FL time is given by $\tau_{single}^{FL} = \max_{k\in\mathcal{K}} \tau_k + T_{diss}$. Thus, the hovering energy consumption of the k-th UAV is obtained as $E_k^{hov} = p^{hov}\tau_{single}^{FL}$. Meanwhile, the transition energy consumption of the k-th UAV is obtained as $E_k^{trans} = P_{trans}\frac{d}{v}$ where P_{trans} is the hardware power consumption for moving UAV, d is the distance between two hovering points, and v is the UAV speed [41]. Without loss of generality, we consider that the UAVs have given trajectories and the distance between two neighboring points in these trajectories is same. Consequently, the transition energy consumption can be considered as a constant. Overall, the k-th UAV's mechanical energy consumption at one global FL iteration is obtained as $E_k^{meh} = E_k^{hov} + E_k^{trans}$.
- *UAV's communication energy consumption:* The consumed energy for transmitting the local aggregated models back to the associated UDs can be denoted by E_k^{com} and calculated as $E_{k,1}^{com} = PT_k^{do}$. Meanwhile, the energy consumed for disseminating model parameters is obtained $E_{k,2}^{com} = PT_{diss}$. Thus, the total communication energy consumed at the k-th UAV for one global FL iteration is $E_k^{com} = E_{k,1}^{com} + E_{k,2}^{com}$.

The overall energy consumption of the k-th UAV in one global FL iteration is obtained as $E_k^{meh} + E_k^{com}$, $\forall k$. Accordingly, the overall energy consumption of the k-th UAV and the u-th UD for all global iterations T, $\forall k$ and $\forall u$, respectively, are obtained as

$$E_k = T\left(E_k^{meh} + E_k^{com}\right), E_u = T\left(E_u^{comp} + E_u^{com}\right). \tag{11}$$

B. PROBLEM FORMULATION

Given the ATIN and its FL time and energy components, our next step is to formulate the energy consumption minimization problem that involves the joint optimization of two sub-problems, namely UAV-LOS UD clustering and D2D scheduling sub-problems. To minimize the energy consumption at each global iteration, we need to develop a framework that decides: i) the UAV-UD clustering; ii) the adopted transmission rate of the UDs $\mathcal{U}_{los}$ to transmit their local models to the set of UAVs/RRBs; and iii) the set of D2D transmitters (relays) that helping the non-LOS UDs to transmit their local models to the set of UAVs $\mathcal{K}$. As such, the local models are delivered to all UAVs with minimum duration time, thus minimum energy consumption for UAV's hovering and UD's wireless transmission. Therefore, the energy consumption minimization problem in the ATIN can be formulated as follows.

$$\text{P0:} \min_{R^u_{min}, \mathcal{U}_{los}, \mathcal{U}_{non}} \sum_{k\in\mathcal{K}} E_k + \sum_{u\in\mathcal{U}} E_u$$
$$\text{s.}t. \begin{cases} \text{C1: } \mathcal{U}_{k,los} \cap \mathcal{U}_{k',los} = \emptyset, \forall (k,k') \in \mathcal{K}, \\ \text{C2: } \mathcal{U}_{k,los} \cap \mathcal{U}_{u',los} = \emptyset, \forall k \in \mathcal{K}, \\ \text{C3: } \mathcal{U}_{u,los} \cap \mathcal{U}_{u'',los} = \emptyset, \\ \text{C4: } R^u_{k,b} \geq R_0, (u,k,b) \in (\mathcal{U},\mathcal{K},\mathcal{B}), \\ \text{C5: } \mathtt{T}_{\hat{u}} \leq T_u, u \in \mathcal{U}_{los}, \\ \text{C6: } T^{\bar{u}}_{idle} \geq (\frac{s}{R^{\bar{u}}_{\hat{u}}} + \frac{s}{R^{\bar{u}}_{k,b}}), \bar{u} \in \mathcal{U}_{los}, \hat{u} \in \mathcal{U}_{non}, \\ \text{C7: } \tau \leq T_{\max}. \end{cases} \tag{12a}$$

The constraints are explained as follows. Constraint C1 states that the set of scheduled UDs to the UAVs are disjoint, i.e., each UD must be scheduled to only one UAV. Constraints C2 and C3 make sure that each UD can be scheduled to only one relay and no UD can be scheduled to a relay and UAV at the same time instant. Constraint C4 is on the coverage threshold of each UAV. Constraint C5 ensures that the local parameters of UD $\hat{u}$ has to be delivered to UAV k via relay $\bar{u}$ within $\frac{s}{R^u_{min}}$, i.e., $\mathtt{T}_{\hat{u}} = \frac{s}{R^{\bar{u}}_{\hat{u}}} + \frac{s}{R^{\bar{u}}_{k,b}} \leq \frac{s}{R^u_{min}}$. Constraint C6 ensures that the idle time of UD $\bar{u}$ is long enough for transmitting the local parameters of UD $\hat{u}$ to UAV k. Constraint C7 is for the FL time threshold T_{max}. Problem P0 is provably NP-hard. However, by analyzing the problem, we can decompose it into two sub-problems and solve them individually and efficiently.

Remark 3: In this work, we develop a novel FedMoD FL that includes (i) the design of the introduced decentralized FL framework, (ii) its convergence analysis, and (iii) an optimization objective to assess the performance of the proposed decentralized FedMoD framework as compared to conventional FL schemes, e.g., HFL and star-based FL schemes, which is non-trivial due to the following reason. The considered realistic UAV topology requires careful optimization over these two main factors: (i) the scheduling of LOS UDs to suitable UAVs and RRBs over mmWave links and (ii) the scheduling of non-LOS UDs to LOS UDs over side-link D2D communications such that non-LOS can transmit their model parameters to UAVs with the help of available LOS UDs. On the one hand, such joint factors need to be carefully optimized to form a dynamic clustering topology at each global iteration. Thus, the optimization problem P0 does not contain an FL accuracy constraint. The joint optimization of both RRM and FL accuracy is appealing and can be considered in our future work.

Remark 4: As mentioned in Section IV-A(2) that the UAVs need to remain stationary at the air for the entire duration of each global FL iteration to perform model parameter aggregation and dissemination. Therefore, the UAVs' mechanical energy consumption (and thus, the overall system energy consumption) directly depends on the time required to complete one single global FL iteration. Accordingly, the system's energy consumption can be reduced by minimizing the FL time, which in turn depends on the time required for uploading model parameters from the scheduled UDs to the associated UAVs. Consequently, in this work, we optimize the scheduling of the LOS UDs to the UAVs and non-LOS UDs to the LOS UDs as such the required time to complete each global FL iteration is maintained and thereby, the energy consumption is reduced.

C. PROBLEM DECOMPOSITION

First, we focus on minimizing the energy consumption via efficient RRM scheduling of UDs $\mathcal{U}_{los}$ to the UAVs/RRBs. In particular, we can get the possible minimum transmission duration of UD $u \in \mathcal{U}_{los}$ by jointly optimizing the UD scheduling and rate adaptation in $\mathcal{U}_{los}$. The mathematical formulation for minimizing the energy consumption via minimizing the transmission durations for UDs-UAVs/RRBs transmissions can be expressed as

$$\text{P1:} \min_{R^u_{min}, \mathcal{U}_{los}} \sum_{k\in\mathcal{K}} E_k + \sum_{u\in\mathcal{U}} E_u$$
$$\text{s.}t. \left\{ \text{(C1)}, \quad \text{(C4)}, \quad \text{(C5)}, \quad \text{(C7)}. \right. \tag{13a}$$

Note that this sub-problem contains UD-UAV/RRB scheduling and an efficient solution will be developed in Section V-A.

After obtaining the possible transmission duration from UD-UAV transmissions, denoted by T_u of the u-th UD ($u \in \mathcal{U}_{los}$), by solving P1, we can now formulate the second sub-problem. In particular, we can minimize the energy consumption of non-LOS UDs $\mathcal{U}_{non}$ that are not been scheduled to the UAVs within T_u by using D2D communications via relaying mode. For this, UDs being scheduled to the UAVs from sub-problem P1 can be exploited as relays and schedule non-LOS UDs on D2D links within their idle times. Therefore, the second sub-problem of minimizing the energy consumption of unscheduled UDs to be scheduled on D2D links via relaying mode can be expressed as P2 as follows

$$\text{P2:} \min_{\mathcal{U}_{non}} \sum_{k\in\mathcal{K}} E_k + \sum_{u\in\mathcal{U}} E_u$$
$$\text{s.}t. \begin{cases} \text{(C2)}, \quad \text{(C3)}, \quad \text{(C5)}, \quad \text{(C6)} \\ \text{C8: } \mathcal{U}_{non} \in \mathcal{P}(\mathcal{U} \backslash \mathcal{N}_{los}). \end{cases} \tag{14a}$$

Constraint C8 states that the set of relays is constrained only on the UDs that are not been scheduled to the UAVs. It can be easily observed that P2 is a D2D scheduling problem that considers the selection of relays and their non-LOS scheduled UDs.

V. ENERGY-EFFICIENT FedMoD: PROPOSED SOLUTIONS TO P1 AND P2

The proposed FedMoD framework has three sequential procedures as follows: (i) LOS UDs to UAVs scheduling for local models upload, (ii) non-LOS UDs to LOS UDs (called relays) scheduling for D2D communications and local models upload, and (iii) UAV-UAV communications for local aggregated models dissemination. Those three procedures can be executed in a (i) centralized manner, where the CPS does a seamless integration and coordination between UAVs and D2D systems or (ii) distributed way, where UAVs can collect local information from the UDs under their coverage for local model upload and collect local information from their adjacent UAVs for model dissemination. In this work, we propose a robust and efficient semi-centralized FL mechanism of the above mentioned procedures to ensure seamless integration and coordination between UAVs and D2D systems as follows. In particular, procedures 1 and 2 are executed at the CPS, which will be presented in Section V-A and Section V-B, respectively. Procedure 3 is executed in a distributed manner as presented in Algorithm 1. When the UAVs complete the global model aggregation, they send the aggregated model back to the UDs to start a new global learning iteration. Meanwhile, the UAVs inform the CPS via mmWave links to start the scheduling procedures 1 and 2.

The overall solution of solving the two subproblems is presented in Fig. 3.

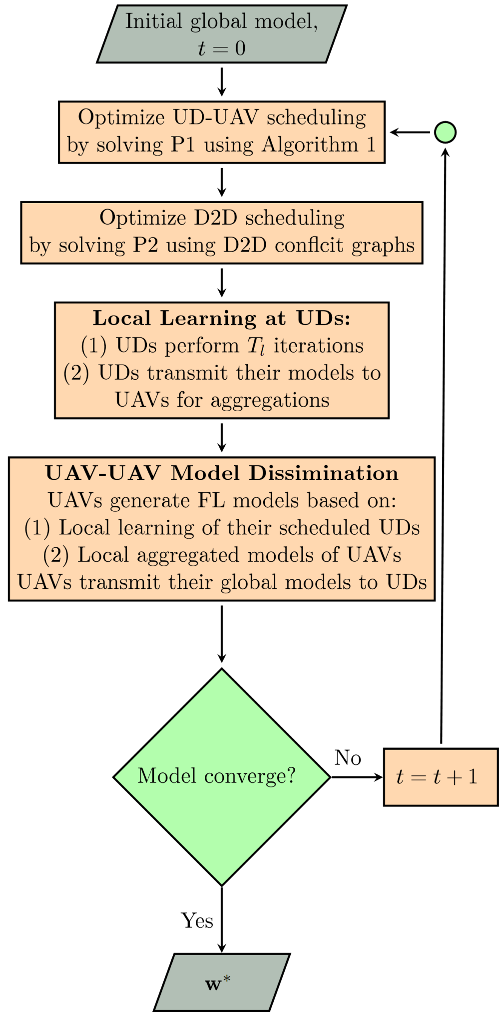

FIGURE 3. The flowchart for the proposed FedMoD.

A. SOLUTION TO SUBPROBLEM P1: UAV-UD CLUSTERING

We exploit a conflict-graph theoretic approach to solve P1 efficiently.[1] We first construct a conflict graph. To this end, the set of all possible associations between UAVs, RRBs, and LOS UDs is denoted by $\mathcal{A}$, which is defined as $\mathcal{A} = \mathcal{K} \times \mathcal{B} \times \mathcal{U}_{los}$. A single association a in the set $\mathcal{A}$ can be represented as (k, b, u), where k represents a UAV, b represents an RRB, and u represents a UD. The conflict clustering graph in the network is represented by $\mathcal{G}(\mathcal{V}, \mathcal{E})$, where $\mathcal{V}$ and $\mathcal{E}$ are the sets of vertices and edges of $\mathcal{G}$, respectively. In this graph, each vertex represents an association in set $\mathcal{A}$, and every edge between two different vertices represents a conflict connection between the two corresponding associations of the vertices, according to C1 in P1. The conflict clustering graph is constructed by generating a vertex $v \in \mathcal{V}$ associated with $a \in \mathcal{A}$ for UDs that have enough energy to perform learning and wireless transmissions. To select the UD-UAV-RRB scheduling that provides a minimum energy consumption while ensuring C4 and C7 constraints in P1, a weight $w(v)$ is assigned to each vertex $v \in \mathcal{V}$. For simplicity, the weight of vertex $v^b_{k,u}$ is defined as $w(v^b_{k,u}) = E^{comp}_u + E^{com}_u$. Two vertices $v^b_{k,u}$ and $v^{b'}_{k',u'}$ are conflicting vertices that will be connected by an edge in $\mathcal{E}$ if one of the following connectivity conditions (CC) is satisfied.

- **CC1:** ($u = u'$ and $b = b'$ or $k = k'$). **CC1** states that the same user u is in both vertices $v^b_{k,u}$ and $v^{b'}_{k',u'}$.
- **CC2:** ($b = b'$ and $u \neq u'$). **CC2** implies that the same RRB is in both vertices $v^b_{k,u}$ and $v^{b'}_{k,u'}$.

Note that the violation of constraint C1 in problem P1 is represented by connectivity conditions **CC1** and **CC2**. Essentially, two vertices are in conflict with each other if (i) they contain the same UD that is associated with different UAVs or RRBs, or (ii) they contain the same RRB that is associated with different UDs. We emphasize that the conflict clustering graph designed for solving P1 has several similarities with the MWIS problem. For example, in both P1 and MWIS, two non-adjacent vertices are required (according to **CC1** and **CC2** conditions) and in P1, the same local learning user cannot be scheduled to multiple UAVs or RRBs as per the constraint C1. Moreover, energy consumption minimization

[1] Note that the conflict-graph theory was also exploited in [28]. However, different from [28], (i) we exploit UAV-to-UAV and D2D scheduling for developing a decentralized model dissemination scheme in mmWave ATINs, and (ii) the focus of the current work is to minimize the network's energy consumption for FL while [28] considered maximizing the secrecy rate in FL. Despite adopting a similar method to solve the resource optimization problem, our considered FL problem is entirely different from [28].

is the objective of problem P2 in ATIN, which is also the same as the goal of MWIS to select a number of vertices with small weights. Motivated by such similarity between the MWIS and P1, the solution to P1 is characterized by the following theorem.

Theorem 1: The solution to problem P1 is equivalent to the minimum independent set weighting-search method, in which the weight of each vertex v corresponding to UD u is

$$w(v) = E_u^{comp} + E_u^{com}. \tag{15}$$

In what follows, we provide a sketch on finding MWIS set Γ^* among all other minimal sets in the $\mathcal{G}$ graph. At first, we select vertex $v_i \in \mathcal{V}, (i = 1, 2, \cdots,)$ that has the minimum weight $w(v_i^*)$ and add it to Γ^* (at this point, $\Gamma^* = \{v_i^*\}$). Subsequently, the subgraph $\mathcal{G}(\Gamma^*)$, which consists of vertices in graph $\mathcal{G}$ that are not adjacent to vertex v_i^*, is extracted and considered for the next vertex selection process. Thereafter, we select a new minimum weight vertex $v_{i'}^*$ (i.e., $v_{i'}^*$ should be in the corresponding set of v_i^*) from subgraph $\mathcal{G}(\Gamma^*)$. Consequently, the set Γ^* is updated as $\Gamma^* \leftarrow \{v_i^*, v_{i'}^*\}$. We repeat the aforementioned process until no further vertex is adjacent to all vertices in Γ^*. Note that at most BK vertices can be selected, and the final MWIS set is therefore denoted by $\Gamma^* = \{v_1^*, v_2^*, \cdots, v_{BK}^*\}$. We emphasize that such an MWIS set represents a feasible UD-UAV/RRB scheduling solution to P1.

B. SOLUTION TO SUBPROBLEM P2: D2D GRAPH CONSTRUCTION

In this subsection, our main focus is to schedule the non-LOS UDs to the LOS UDs (relays) over their idle times so that the local models of those non-LOS UDs can be forwarded to the UAVs. Since the non-LOS UDs communicate with their respective relays over D2D links, the D2D connectivity can be characterized by an undirected graph $\mathcal{G}(\mathcal{V}, \mathcal{E})$ with $\mathcal{V}$ denoting the set of vertices and $\mathcal{E}$ the set of edges. We construct a new D2D conflict graph that considers all possible conflicts for scheduling non-LOS UDs on D2D links, such as transmission and half-duplex conflicts. This leads to feasible transmissions from the potential D2D transmitters $|\mathcal{U}_{\text{non,tra}}|$.

Recall $\mathcal{U}_{\text{non}}$ is the set of non-LOS UDs, i.e., $\mathcal{U}_{\text{non}} = \mathcal{U} \backslash \mathcal{U}_{los}$, and let $\mathcal{U}_{\text{relay}} = \mathcal{U}_{\text{los}} \backslash \{u\}$ denote the set of relays that can use their idle times to help the non-LOS UDs. Hence, the D2D conflict graph is designed by generating all vertices for $\bar{u}$-th possible relay, $\forall \bar{u} \in \mathcal{U}_{\text{relay}}$. The vertex set $\mathcal{V}$ of the entire graph is the union of vertices of all users. Consider, for now, generating the vertices of the $\bar{u}$-th relay. Note that $\bar{u}$-th relay can help one non-LOS UD as long as it is in the coverage zone and is capable of delivering the local model to the scheduled UAV within its idle time. Therefore, each vertex is generated for each single non-LoS UD that is located in the coverage zone of the $\bar{u}$-th relay and $\mathtt{T}_{\hat{u}} \leq T_{idle}^{\bar{u}}$. Accordingly, the i-th non-LOS UD in the coverage zone $\mathcal{Z}_{\bar{u}}$ can transmit its model to the $\bar{u}$-th relay. Therefore, we generate $|\mathcal{Z}_{\bar{u}}|$ vertices for the $\bar{u}$-th relay.

All possible conflict connections between vertices (conflict edges between circles) in the D2D conflict graph are provided as follows. Two vertices $v_i^{\bar{u}}$ and $v_{i'}^{u'}$ are adjacent by a conflict edge in $\mathcal{G}_{\text{d2d}}$, if one of the following conflict conditions is true: (i) $(\bar{u} \neq u')$ and $(i = i')$. The same non-LoS UD cannot be scheduled to two different helpers $\bar{u}$ and u'. (ii) $(i \neq i')$ and $(\bar{u} = u')$. Two different non-LoS UDs can not be scheduled to the same relay. These two conditions represent C3 in P2, where each non-LoS UD must be assigned to one relay and the same relay cannot accommodate more than one non-LoS UD. Given the aforementioned designed D2D conflict graph, the following theorem reformulates the subproblem P2.

Theorem 2: The subproblem of scheduling non-LOS UDs on D2D links in P2 is equivalently represented by the MWIS selection among all the maximal sets in the $\mathcal{G}_{d2d}$ graph, where the weight $\psi(v_i^{\bar{u}})$ of each vertex $v_i^{\bar{u}}$ is given by $\psi(v_i^{\bar{u}}) = r$.

Since P2 is also equivalent to an MWIS selection problem, its solution can be obtained using a similar method detailed at the end of Section V. A. Due to the space limitations, the repeated discussion is omitted.

C. COMPUTATIONAL COMPLEXITY

Let $U_{\text{inv}}^{\text{star}} = \min(U, B)$, $U_{\text{inv}}^{\text{HFL}}$, and $U_{\text{inv}}^{\text{FedMoD}}$ be the number of involved UDs in the learning of the star-based, HFL, and FedMoD FL schemes, respectively. Note that since the global model aggregation is just an averaging of all the trained local models of the involved UDs, its computational complexity can be ignored for all the schemes. The star-based requires a computational complexity of CPS/RRB-UD scheduling, which requires $\mathcal{O}\big(U_{\text{inv}}^{\text{star}}\big)$ operations. On the other hand, it requires a computational complexity for local learning at the UDs, which is $\mathcal{O}(U_{\text{inv}}^{\text{star}} f(S))$, where $f(S)$ is the complexity of ML solver with S dataset, which holds for all schemes. Such computational complexity depends on dataset type. Thus, the total computational complexity of the star-based FL is $O\big(T(U_{\text{inv}}^{\text{star}} + U_{\text{inv}}^{\text{star}} f(S))\big)$ operations. The computational complexity of the proposed FedMoD is explained as follows. First, we consider an MWIS greedy search for the following scheduling procedures: (i) UD-UAV, (ii) D2D links, and (iii) UAV-UAV, where its computational complexity depends on vertex generation and graph construction. In particular, the MWIS solution for UD-UAV scheduling requires generating a maximum of $\mathcal{O}(U_{\text{los}}KB)$ vertices, calculating their weights requires $\mathcal{O}(U_{\text{los}}KB)$, and connecting those vertices requires $\mathcal{O}(U_{\text{los}}^2 K^2 B^2)$ [28], which yields the worst-case complexity of $\mathcal{O}(U_{\text{los}}^2 K^2 B^2)$. Next, the MWIS solution for LOS-non-LOS scheduling requires generating a maximum of $\mathcal{O}(U_{\text{relay}} U_{\text{non}})$ vertices, calculating their weights requires $\mathcal{O}(U_{\text{relay}} U_{\text{non}})$, and connecting those vertices requires $\mathcal{O}(U_{\text{relay}}^2 U_{\text{non}}^2)$ [28], which yields the worst-case complexity of $\mathcal{O}(U_{\text{relay}}^2 U_{\text{non}}^2)$. Next, the MWIS solution for UAV-UAV scheduling requires generating a maximum of $\mathcal{O}(K^2)$ vertices, calculating their weights requires $\mathcal{O}(K^2)$, and connecting those vertices requires $\mathcal{O}(K^2)$ [28], which yields the worst-case complexity of $\mathcal{O}(3K^2)$. Then, in each greedy iteration of each of the above procedures, respectively, we select one vertex up to a maximum U_{los}, K, and U_{relay} vertices. We combine all the complexities of the different solution elements including the learning part, which yields the total complexity of the FedMoD of $\mathcal{O}\big(T(U_{\text{los}}^2K^2B^2 + U_{\text{relay}}^2U_{\text{non}}^2 + 3K^2 + U_{\text{los}} + U_{\text{relay}} + K + U_{\text{inv}}^{\text{FedMoD}}f(S))\big) = \mathcal{O}\big(T(U_{\text{los}}^2K^2B^2 + U_{\text{relay}}^2U_{\text{non}}^2 + U_{\text{inv}}^{\text{FedMoD}}f(S))\big)$. Similarly, the HFL requires a computational complexity of UAV/RRB-UD scheduling only and local learning, which requires $\mathcal{O}\big(T(U^2K^2B^2 + U_{\text{inv}}^{\text{HFL}}f(S))\big)$ arithmetic operations. Notably, star-based FL requires low computational complexity than HFL and FedMoD, and FedMoD is better than HFL since the greedy search of HFL is over all the UDs in the network, opposed to FedMoD that is over LOS UDs only. This observation can be seen in the running time of Table 2 in the numerical section, where HFL requires more computing time than star-based and FedMoD.

VI. PERFORMANCE EVALUATION

A. SIMULATION SETTING

For our simulations, a circular network area having a radius of 400 meter (m) is considered. The height of the CPS is 10 m [2]. Unless specified otherwise, we divide the considered circular network area into 5 target locations. As mentioned in the system model, each target location is assigned to one UAV, and the locations of the UAVs are randomly distributed in the flying plane with an altitude of 100 m. The users are placed randomly in the area. In addition, U users are connected to the UAVs through orthogonal RRBs for uplink local model transmissions. The bandwidth of each RRB is 2 MHz. The UAV communicates with the neighboring UAVs via high-speed mmWave communication links [26], [35].

Our proposed FedMoD scheme is evaluated on the MNIST and CIFAR-10 datasets, which are well-known benchmark datasets for image classification tasks. Each image is one of 10 categories. We divide the dataset into the UDs' local data $\mathcal{D}_u$ with non-i.i.d. data heterogeneity, where each local dataset contains data points from two of the 10 labels. In each case, $\mathcal{D}_u$ is selected randomly from the full dataset of labels assigned to the u-th UD. We also assume non-iid-clustering, where the maximum number of assigned classes for each cluster is 6 classes. For ML models, we use a deep neural network with 3 convolutional layers and 1 fully connected layers. The total number of trainable parameters for MNIST is $9,098$ and for CIFAR-10 is $21,840$. We simulate a FedMoD system with 30 UDs (for CIFAR-10) and 20 UDs (for MNIST) and 5 UAVs each with 7 orthogonal RRBs. In our experiments, we consider a network topology that is illustrated in Fig. 11 unless otherwise specified. The remaining simulation parameters are summarized in TABLE 1 and selected based on [2], [33], [38], and [41]. To showcase the effectiveness of FedMoD in terms of learning accuracy and energy consumption, we consider the *Star-based FL* and *HFL* schemes.

TABLE 1. **Simulation parameters.**

Parameter	Value
Carrier frequency, f	1 GHz [2]
Speed of light, c	3×10^8 m/s
UAV's and UD's transmit maximum powers, P, p	1 Watt and 3 Watt [2]
Transmit power of the CPS	5 Watt
Noise PSD, N_0	-174 dBm/Hz
Local and aggregated parameters size, s	9.1 KB
UD processing density, Q_u	$[400 - 600]$
UD computation frequency, f_u	$[0.0003 - 1]$ G cycles/s
CPU architecture based parameter, α_c	10^{-28}
FL time threshold T_{max}	1 Second
Number of data samples, D_u	200

B. FedMoD's ACCURACY AND CONVERGENCE PERFORMANCE

We show the training accuracy with respect to number of iterations for both the MNIST and CIFAR-10 datasets with different model dissemination rounds α in Fig. 4. Specially, in Figs. 4(a) and 4(b), we show the accuracy performance of our proposed FedMoD scheme with full dissemination against the centralized FL schemes. Particularly, in the considered star-based and HFL schemes, the CPS can receive the local trained models from the UDs, where each scheduled UD transmits its trained model directly to the CPS (in case of star-based FL) or through UAVs (in case of HFL). Thus, the CPS can aggregate all the local models of all the scheduled UDs. In the considered decentralized FedMoD, before the dissemination rounds start, each UAV has aggregated the trained local models of the scheduled UDs in its cluster only. However, with the novel dissemination FedMoD method, each UAV shares its aggregated models with the neighboring UAVs using one-hop transmission. Thus, at each dissemination round, UAVs build their side information (*Known* models and *Unknown* models) until they receive all the *Unknown* models. Thus, the UAVs have full knowledge of the global model of the system at each global iteration. Thanks to the efficient FedMoD dissemination method, the accuracy of the proposed FedMoD scheme is almost the same as the centralized FL schemes. Such efficient communications among UAVs accelerate the learning progress, thereby FedMoD model reaches an accuracy of (0.945, 0.668 for MNIST and CIFAR-10) with around 200 and 300 global iterations, respectively, as compared to the accuracy of (0.955, 0.944 for MNIST) and (0.665, 0.668 for CIFAR-10) for star-based and HFL schemes, respectively. It is important to note that although our proposed scheme overcomes the struggling UD issue of the star-based scheme and the two-hop transmission of the HFL, it needs a few rounds of model dissemination. However, the effective coding scheme of the models minimizes the number of dissemination rounds. In addition, due to the high communication links between the UAVs, the dissemination delay is negligible which does not affect the FL time.

In Figs. 5(a) and 5(b), we further study the impact of the number of dissemination rounds α on the convergence

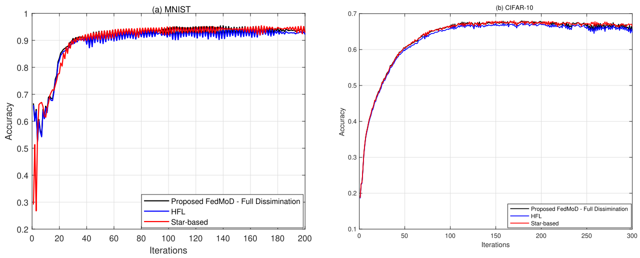

FIGURE 4. Performance comparison between FedMoD and baseline schemes for MNIST and CIFAR-10: Accuracy vs. number of iterations.

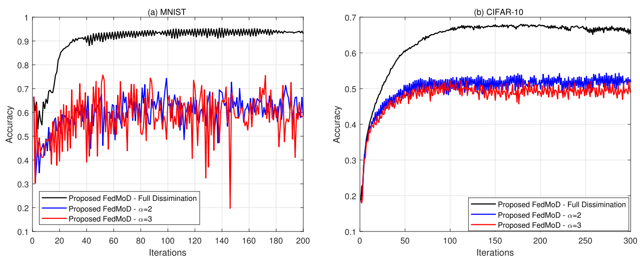

FIGURE 5. Performance comparison of FedMoD for MNIST and CIFAR-10 with different α.

rate of the proposed FedMoD scheme for both the MNIST and CIFAR-10 datasets. For both figures, we consider the following three proposed schemes: (i) FedMoD scheme-full dissemination where UAVs perform full model dissemination at each global iteration, (ii) FedMoD scheme - $\alpha = 2$ where partially dissemination is performed and after each 2 complete global iterations, we perform full dissemination, and (iii) FedMoD scheme - $\alpha = 3$ where partially dissemination is performed and after each 3 complete global iterations, full dissemination is performed. From Figs. 5(a) and 5(b), we observe that partial dissemination with less frequent full dissemination leads to a lower training accuracy within a given number of training iterations. Specifically, the accuracy performance for full dissemination, $\alpha = 2$ and 3 schemes is $0.966, 0.66, 0.75$ for MNIST and $0.668, 0.52, 0.59$ for CIFAR-10, respectively. Infrequent inter-cluster UAV dissemination also leads to unstable convergence since the UAVs do not frequently aggregate all the locally trained models of the UDs.

In Fig. 6, we plot the accuracy of the proposed and benchmark schemes versus the number of global iterations for 28 UDs and 20 RRBs. In Fig. 6, we perform the simulations on CIFAR-10 dataset and consider a practical model, where the number of available RRBs is less than the number of UDs. Similar to the discussion of Fig. 4(b), at the beginning of the learning, the BS aggregates all the local models and reaches accuracy of 60% and 56% with around 50 global iterations for star-based and HFL schemes, respectively. The proposed FedMoD, at the beginning, has limited knowledge on the global model since it only knows the local model that depends on its scheduled UDs in the corresponding cluster.

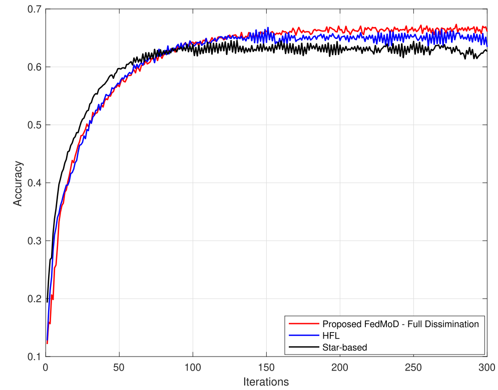

FIGURE 6. Accuracy vs. number of global iterations for a network configuration of 28 UDs and 20 RRBs.

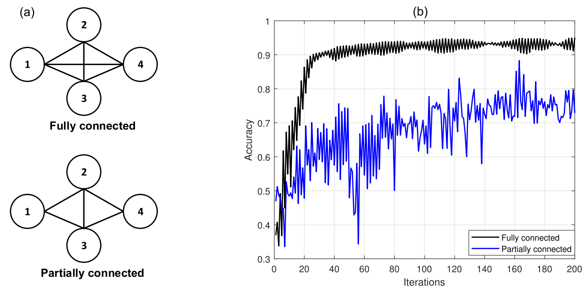

FIGURE 7. Typical network topologies of the UAVs for model dissemination and their FL accuracy.

Consequently, it has a low accuracy of 55% at 50 iterations compared to the aforementioned schemes. However, using the efficient dissemination scheme between the UAVs, the proposed FedMoD algorithm effectively disseminates the aggregated models of UAVs to their adjacent clusters. With increasing the number of iterations, the UAVs have better knowledge about the global model of the system. Thus, the accuracy of our proposed FedMoD scheme is effectively increased with the number of rounds. Therefore, as can be seen from Fig. 6, the proposed scheme has better accuracy than the HFL scheme at convergence of 300 rounds, and both have improved performances as compared to the star-based FL scheme. Due to the RRB allocation reusing scheme among the UAVs, the number of involved UDs in the learning of the proposed and HFL schemes is larger than of the star-based-scheme. In fact, the number of involved UDs in the proposed and HFL schemes can reach up to 28 UDs, while the number of scheduled UDs in the start-based scheme is maintained by the total number of the available RRBs in the system, which is 20 UDs.

C. IMPACT OF NETWORK TOPOLOGY AND FedMoD's ENERGY EFFICIENCY

We also evaluate the learning accuracy of FedMoD on different network topologies of the UAVs as shown in Fig. 7(a). We consider a fully connected network where all the UAVs are connected and a partially connected network where UAV

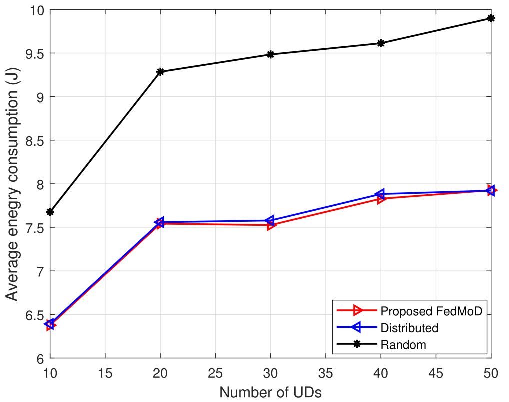

FIGURE 8. **Average energy consumption vs. number of UDs.**

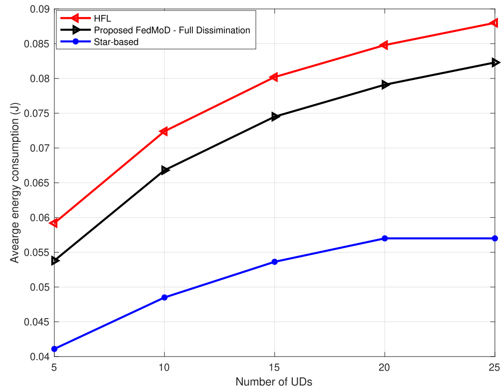

FIGURE 9. **Average energy consumption vs. number of UDs for 20 RRBs.**

4 is not connected to UAV 1. In this figure, we perform 4 different rounds of dissemination. As shown in Fig. 7(b), we see that within a given number of global iterations, a more connected network topology achieves a higher test accuracy. This is because more model information is collected from neighboring UAVs in each round of inter-UAV model aggregation. It is also observed that when α is greater than 4, the test accuracy of the partially connected network can approach the case with a fully connected network. Therefore, based on the network topology of UAVs, we can choose a suitable value of α to balance between the number of inter-cluster UAV aggregation and learning performance.

In Fig. 8, we plot the energy consumption of the proposed and benchmark schemes versus the number of UDs for a network of 4 UAVs and 4 RRBs per UAV. From the objective function of problem P1, we can observe that an efficient radio resource management scheme leads to a lower energy consumption. Hence, from Fig. 8, we observe that for FedMoD, the average energy consumption is minimized. Such an observation is because the proposed schemes judiciously allocate LOS UDs to the UAVs and their available RRBs as well as D2D communications. In particular, the random scheme has the largest energy consumption because it randomly schedules the UDs to the UAVs and their available RRBs. Accordingly, from energy consumption perspective, it is inefficient to consider a random radio resource management scheme. From Fig. 8, it is observed that the proposed centralized scheduling FedMoD and distributed FedMoD schemes offer the same energy consumption performances for the same number of UDs. Such an observation can be explained by the following argument. When we have a large number of UDs, the probability that a UD is scheduled for more than one UAV decreases. As a result, the conflict among UAVs and the likelihood of scheduling UDs to the wrong UAV decreases. As an insight from this figure, a distributed radio resource management scheme is a suitable alternative for scheduling the LOS UDs to the UAVs, especially for large-scale networks.

To further study the performance of the proposed scheme, in Fig. 9, we plot the energy consumption of the proposed and benchmark schemes versus the number of UDs for 20 RRBs. Fig. Fig. 9 depicts that the star-based FL has improved performance in terms of energy consumption compared to the HFL and FedMoD. This is because the UAVs in HFL and FedMoD need to hover to (1) collect the local models of the UDs and (2) disseminate their local aggregated models to other UAVs to reach the global model without the need for global model aggregator of the star-based. Such UAVs hovering consumes more energy. Besides the impact of the UAVs hovering on the energy consumption, the number of involved UDs plays a vital role in the energy consumption. Since the proposed FedMoD and HFL can accommodate more scheduled UDs than the star-based FL, due to reusing the available resources among different UAVs, the consumed energy is increased. However, as depicted in Fig. 9(a), increasing the number of UDs in the learning leads to improve the learning accuracy, and both schemes work better than the star-based in terms of learning accuracy. Our proposed FedMoD strikes a balance between these benchmark schemes by (i) augmenting the need for two hops of transmission of the HFL; and (ii) ensuring short range communications between the UAVs and scheduled UDs (unlike the star-based FL that requires a distant CPS). Thus, it has improved performance compared to the HFL.

In Fig. 10, we evaluate the energy consumption (dash lines) and number of scheduled UDs (solid lines) of the proposed FedMoD and benchmark schemes by changing the number of RRBs in a network of 40 UDs. From Fig. 10, we observe that the number of scheduled UDs of star-based FL is equal to the number of RRBs in the system. In particular, when the total number of RRBs is nearly 25, the effective system capacity of the star-based FL stops growing and can have at most 25 scheduled UDs. Therefore, the star-based FL is impractical in terms of the number of scheduled UDs, particularly for massive networks with limited radio resources. However, in the considered UAV schemes (i.e., FedMoD and HFL), the set of RRBs can be re-used among non-adjacent clustering UAVs. As a result, the number of scheduled UDs of the considered D2D schemes is increased. Indeed, Fig. 10

TABLE 2. Execution time (in seconds) of the simulated schemes and their computational complexity.

Schemes	Number of UDs				Computational Complexity
	15	25	35	45	
FedMoD	0.024988	0.056454	0.0584148	0.0595513	$\mathcal{O}\big(T(U_{\text{los}}^2 K^2 B^2 + U_{\text{relay}}^2 U_{\text{non}}^2 + U_{\text{inv}}^{\text{FedMoD}} f(S))\big)$
HFL	0.030025	0.061745	0.070445	0.078199	$\mathcal{O}\big(T(U^2 K^2 B^2 + U_{\text{inv}}^{\text{HFL}} f(S))\big)$
Star-based	0.002789	0.004731	0.005734	0.005834	$O\big(T(U_{\text{inv}}^{\text{star}} + U_{\text{inv}}^{\text{star}} f(S))\big)$

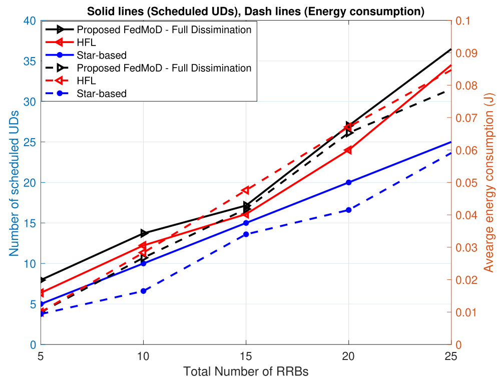

FIGURE 10. Average energy consumption vs. number of RRBs for 40 UDs.

(solid lines) shows that UAV schemes achieve more than 25% improvement in the number of scheduled UDs compared to the star-based FL for 40 UDs and 25 RRBs in the network. On the other hand, the energy consumption (dash lines) of the FedMoD and HFL is degraded compared to the star-based due the following argument. First, the FedMoD offloads the CPS to perform any global model aggregation, however it consumes more energy for UAV hovering. Second, the number of scheduled UDs (solid lines) plays a vital role in the energy consumption. Since the proposed FedMoD and HFL can accommodate more scheduled UDs than the star-based FL, due to reusing the available resources among different UAVs, the consumed energy is increased. However, increasing the number of UDs in the learning leads to improve the learning accuracy as depicted in Fig. 6. Thus, both schemes work better than the star-based in terms of learning accuracy.

Finally, Table 2 provides the run time of MATLAB for all the proposed schemes for one global iteration. We consider a network setup of 3 UAVs and different number of UDs. Table 2 shows that HFL scheme requires high computation time than all the other solutions. This is due to the fact that HFL searches all the possible UD-UAV/RRB associations in the network. Star-based scheme has low computing time, but it relies on the CPS for scheduling and global aggregations. It also does not converge well in massive networks, where there is a large number of UDs with limited number of RRBs in the network. Thus, our proposed FedMoD scheme can be executed quickly without the need for the CPS's global aggregations, making it preferred method for application in UAV networks.

VII. CONCLUSION

In this paper, we developed a novel decentralized FL scheme, called FedMoD, which maintains convergence speed and reduces the energy consumption of FL in mmWave ATINs. Specifically, we proposed a FedMoD scheme based on inter-cluster UAV communications and theoretically proved its convergence. A rate-adaptive and D2D-assisted RRM scheme was also developed to minimize the overall energy consumption of the proposed decentralized FL scheme. The presented simulation results revealed that our proposed FedMoD achieves the same accuracy as the baseline FL scheme while substantially reducing energy consumption for convergence. In addition, simulation results reveal various insights concerning how the topology of the network impacts the number of inter-cluster UAV aggregations required for the convergence of FedMoD.

APPENDIX A ILLUSTRATION OF THE PROPOSED MODEL DISSEMINATION METHOD

For further illustration, we explain the dissemination method that is implemented at the UAVs through an example of the network topology of Fig. 11. Suppose that all the UAVs have already received the local models of their scheduled UDs and performed the local model averaging. Fig. 11 presents the side information status of each UAV at round $l = 0$.

Round 1: Since UAV 2 has good reachability to many UAVs ($\mathcal{K}_2 = \{1, 4, 3\}$), it transmits its model $\tilde{\mathbf{w}}_{2,0}$ to UAVs 1, 4, and 3 with a transmission rate of $r(l = 1) = \min\{12, 11, 9\} = 9$ Mbps (**CC2** is satisfied). Note that UAV 5 can not transmit to UAV 3 according to **CC3**, i.e., UAV 3 is already scheduled to the transmitting UAV 2. When UAV 2 finishes model transmission, the *Known* sets of the receiving UAVs is updated to $\mathcal{H}_1^1(t) = \{\tilde{\mathbf{w}}_1, \tilde{\mathbf{w}}_2\}$, $\mathcal{H}_3^1(t) = \{\tilde{\mathbf{w}}_3, \tilde{\mathbf{w}}_2\}$, and $\mathcal{H}_4^1(t) = \{\tilde{\mathbf{w}}_4, \tilde{\mathbf{w}}_2\}$. Accordingly, their *Unknown* sets are: $\mathcal{W}_1^1(t) = \{\tilde{\mathbf{w}}_3, \tilde{\mathbf{w}}_4, \tilde{\mathbf{w}}_5\}$, $\mathcal{W}_3^1(t) = \{\tilde{\mathbf{w}}_1, \tilde{\mathbf{w}}_4, \tilde{\mathbf{w}}_5\}$, $\mathcal{W}_4^1(t) = \{\tilde{\mathbf{w}}_1, \tilde{\mathbf{w}}_3, \tilde{\mathbf{w}}_5\}$.

Round 2: Although UAV 2 has good reachability to many UAVs, it would not be selected as a transmitting UAV at $l = 2$. This is because the UAV has already disseminated its side information to the neighboring UAVs. Thus, UAV 2 does not have any vertex in the FedMoD conflict graph. In this case, UAVs 4 and 5 can simultaneously transmit models $\tilde{\mathbf{w}}_4$ and $\tilde{\mathbf{w}}_5$, respectively, to the receiving UAVs $\{1, 2\}$ and $\{3\}$. When UAVs 4 and 5 finish models transmission, the *Known* sets of the receiving UAVs is updated to $\mathcal{H}_1^2(t) = \{\tilde{\mathbf{w}}_1, \tilde{\mathbf{w}}_2, \tilde{\mathbf{w}}_4\}$, $\mathcal{H}_2^2(t) = \{\tilde{\mathbf{w}}_2, \tilde{\mathbf{w}}_4\}$, and $\mathcal{H}_3^2(t) = \{\tilde{\mathbf{w}}_3, \tilde{\mathbf{w}}_2, \tilde{\mathbf{w}}_5\}$. Clearly, UAVs

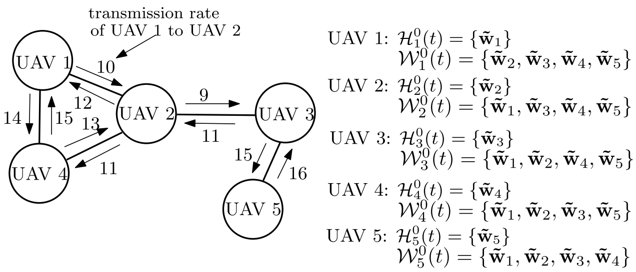

FIGURE 11. A simple example of 5 UAVs with their arbitrary transmission rates and initial side information at round $l = 0$.

4 and 5 transmit their models to the corresponding UAVs with transmission rates of $r_4 = \min\{13, 15\} = 13$ Mbps and $r_5 = 16$ Mbps, respectively. However, for simultaneous transmission and from **CC2**, all the vertices of the corresponding UAVs $\{1, 2, 3\}$ should have the same achievable rate. Thus, UAVs 4 and 5 adopt one transmission rate which is $r(l = 2) = \min\{r_4, r_5\} = 13$ Mbps.

Round 3: UAV 1 transmits model $\tilde{\mathbf{w}}_1$ to the receiving UAVs $\{2, 4\}$, and their *Known* sets are updated to $\mathcal{H}_2^3(t) = \{\tilde{\mathbf{w}}_2, \tilde{\mathbf{w}}_4, \tilde{\mathbf{w}}_1\}$, $\mathcal{H}_4^3(t) = \{\tilde{\mathbf{w}}_4, \tilde{\mathbf{w}}_2, \tilde{\mathbf{w}}_1\}$. UAV 1 transmits its model to the corresponding UAVs with a transmission rate of $r(l = 3) = \min\{10, 14\} = 10$ Mbps.

Round 4: Given the updated side information of the UAVs, UAV 3 can encode models $\tilde{\mathbf{w}}_5$ and $\tilde{\mathbf{w}}_2$ into the encoded model $\tilde{\mathbf{w}}_5 \oplus \tilde{\mathbf{w}}_2$ and broadcasts it to UAVs 2 and 5. Upon reception this encoded model, UAV 5 uses the stored model $\tilde{\mathbf{w}}_5$ to complete model decoding $(\tilde{\mathbf{w}}_5 \oplus \tilde{\mathbf{w}}_2) \oplus \tilde{\mathbf{w}}_5 = \tilde{\mathbf{w}}_2$. Similarly, UAV 5 uses the stored model $\tilde{\mathbf{w}}_2$ to complete model decoding $(\tilde{\mathbf{w}}_5 \oplus \tilde{\mathbf{w}}_2) \oplus \tilde{\mathbf{w}}_2 = \tilde{\mathbf{w}}_5$. The broadcasted model is thus decodable for both UAVs 5 and 2 and has been transmitted with a rate of $r(l = 4) = \min\{11, 15\} = 11$ Mbps. The *Known* sets of these receiving UAVs are as follows: $\mathcal{H}_2^4(t) = \{\tilde{\mathbf{w}}_2, \tilde{\mathbf{w}}_4, \tilde{\mathbf{w}}_1, \tilde{\mathbf{w}}_5\}$ and $\mathcal{H}_5^4(t) = \{\tilde{\mathbf{w}}_5, \tilde{\mathbf{w}}_2\}$.

Round 5: Given the updated side information of the UAVs at $l = 4$, UAV 3 transmits $\tilde{\mathbf{w}}_3$ to UAVs 2 and 5. Upon reception this model, UAV 2 has obtained all the required models, i.e., $\mathcal{H}_2^5(t) = \{\tilde{\mathbf{w}}_1, \tilde{\mathbf{w}}_2, \tilde{\mathbf{w}}_3, \tilde{\mathbf{w}}_4, \tilde{\mathbf{w}}_5\}$ and $\mathcal{W}_2^5(t) = \{\emptyset\}$. The broadcasted model is transmitted with a rate of $r(l = 5) = \min\{11, 15\} = 11$ Mbps. Since UAV 2 has all the local aggregated models of other UAVs, it can aggregate them all which results the global model at the t-th iteration:

$$\tilde{\mathbf{w}}(t) = \frac{1}{D}(\tilde{\mathbf{w}}_1 + \tilde{\mathbf{w}}_2 + \tilde{\mathbf{w}}_3 + \tilde{\mathbf{w}}_4 + \tilde{\mathbf{w}}_5). \tag{16}$$

Therefore, the global model $\tilde{\mathbf{w}}$ is broadcasted from UAV 2 to UAVs $\{1, 4, 3\}$ with a rate of $\min\{12, 11, 9\} = 9$ Mbps. Next, UAV 3 can send $\tilde{\mathbf{w}}$ to UAV 5 with a rate of 15 Mbps. Therefore, all the UAVs obtain the shared global model $\tilde{\mathbf{w}}$ and broadcast it to their scheduled UDs to initialize the next iteration $t + 1$. Note that the transmission duration of these dissemination rounds is

$$T_{diss} = \underbrace{\frac{s}{9}}_{l=1} + \underbrace{\frac{s}{13}}_{l=2} + \underbrace{\frac{s}{10}}_{l=3} + \underbrace{\frac{s}{11}}_{l=4} + \underbrace{\frac{s}{11}}_{l=5} + \underbrace{\frac{s}{9} + \frac{s}{15}}_{\tilde{\mathbf{w}}\text{ broadcasting}}. \tag{17}$$

The size of a typical model is $s = 9.098$ Kb [14], [19], [33], thus $T_{diss} = 0.0059$ sec. Thanks to the efficient model dissemination proposed method that disseminates models from transmitting UAVs to the closest receiving UAVs with good connectivity, the dissemination delay is negligible.

Remark 5: In the fully connected model, each UAV can receive the local aggregated models of all UAVs in K dissemination rounds, where each UAV takes a round for broadcasting its local aggregated model to other UAVs.

APPENDIX B
CONVERGENCE ANALYSIS

Here, we prove the convergence of FedMoD. To facilitate the convergence rate analysis of the proposed scheme, we first provide the following assumptions. For all $u \in \mathcal{U}$, we assume:

1) The local loss function is L-smooth, i.e.,. This assumption implies that for some $L > 0$, $\|\nabla F_u(\mathbf{w}(t + 1)) - \nabla F_u(\mathbf{w}(t))\|_2 \leq L\|\mathbf{w}(t + 1) - \mathbf{w}(t)\|_2$.
2) The mini-batch gradient is unbiased, i.e., $\mathbb{E}_{\mathcal{D}_u|\tilde{\mathbf{w}}} [f(\mathcal{D}_u; \tilde{\mathbf{w}})] = \nabla F_u(\tilde{\mathbf{w}})$, and there exists $\sigma > 0$ such that $\mathbb{E}_{\mathcal{D}_u|\tilde{\mathbf{w}}} \left\| [f(\mathcal{D}_u; \tilde{\mathbf{w}})] - \nabla F_u(\tilde{\mathbf{w}}) \right\|_2^2 \leq \sigma^2$.
3) For the degree of non-IIDness, we assume that there exists $\kappa > 0$ such that $\|\nabla F_u(\tilde{\mathbf{w}}) - \nabla F(\tilde{\mathbf{w}})\|_2 \leq \kappa$, where κ measures the degree of data heterogeneity across all UDs.

In centralized FL, the global model at the CPS at each global iteration evolves according to the following expression [14]:

$$\mathbf{w}(t + 1) = \mathbf{w}(t) - \lambda\mathbf{G}(t), \tag{18}$$

where $\mathbf{w}(t) = [\mathbf{w}_u(t)]_{u\in\mathcal{U}_{inv}}$ and $\mathbf{G}(t) = [g(\mathbf{w}_u(t))]_{u\in\mathcal{U}_{inv}}$. However, in FedMoD, the k-th UAV maintains a model updated based on the trained models of its scheduled UDs only and needs to aggregate the models of other UAVs using the model dissemination method as in Section III-B. Therefore, each UAV has insufficient model averaging unless the model dissemination method is performed until all UAVs obtain the global model defined in (16), i.e., at $l = \alpha$. In other words, at $l = \alpha$, the global model of our proposed decentralized FL should be the one mentioned in (18). For convenience, we define $\tilde{\mathbf{u}}(t) = \sum_{u\in\mathcal{U}_{inv}} m_u\mathbf{w}_u(t)$, and consequently, $\tilde{\mathbf{u}}(t) = \tilde{\mathbf{w}}(t)\mathbf{m}$. By multiplying both sides of the evolution expression in (18) by $\mathbf{m}$, yielding the following expression

$$\tilde{\mathbf{u}}(t + 1) = \tilde{\mathbf{u}}(t) - \lambda\mathbf{G}(t)\mathbf{m}, \tag{19}$$

Following [26] and [27] and leveraging the evolution expression of $\tilde{\mathbf{u}}(t)$ in (19), we bound the expected change of the local loss functions in consecutive iterations as follows.

Lemma 1: The expected change of the global loss function in two consecutive iterations can be bounded as follows

$$\mathbb{E}[F(\tilde{\mathbf{u}}(t+1))] - \mathbb{E}[F(\tilde{\mathbf{u}}(t))] \leq \frac{-\lambda}{2}\mathbb{E}\|\nabla F(\tilde{\mathbf{u}}(t))\|_2^2 + \frac{\lambda^2 L}{2}\sum_{u=1}^{U_{inv}} m_u\sigma^2 - \frac{\lambda}{2}(1-\lambda L)\tilde{Q} + \frac{\lambda L^2}{2}\mathbb{E}\left\|\tilde{\mathbf{w}}(t)(\mathbf{I}-\mathbf{M})\right\|_{\mathbf{M}}^2, \tag{20}$$

where $\tilde{Q} = \mathbb{E}\left[\left\|\sum_{u=1}^{U_{inv}} m_u \nabla F_u(\mathbf{w}_u(t))\right\|_2^2\right]$, $\mathbf{M} = \mathbf{m}\mathbf{I}^T$, *and* $\|\mathbf{X}\|_{\mathbf{M}} = \sum_{i=1}^{M}\sum_{j=1}^{N} m_{i,j}|x_{i,j}|^2$ *is the weighted Frobenius norm of an* $M \times N$ *matrix* $\mathbf{X}$.

For proof, please refer to Appendix C.

Notice that $\tilde{\mathbf{w}}(t)$ deviates from the desired global model due to the partial connectivity of the UAVs that results in the last term in the right-hand side (RHS) of (20). However, through the model dissemination method and at $l = \alpha$, FedMoD ensures that each UAV can aggregate the models of the whole network at each global iteration before proceeding to the next iteration. Thus, such deviation is eliminated.

Due to the model dissemination among the UAVs, there is a dissemination gap that is denoted by the *dissemination gap* between the k-th and j-th UAVs as $\delta_{j,k}(t)$, which is the number of dissemination steps that the local aggregated model of the j-th UAV needs to be transmitted to the k-th UAV. For illustration, consider the example in Fig. 8, the highest dissemination gap is the one between UAVs 5 and 1 which is 3. Thus, $\delta_{5,1}(t) = 3$. The maximum dissemination gap of UAV k is $\delta_k(t) = \max_{j\in\mathcal{K}}\{\delta_{j,k}(t)\}$. Therefore, a larger value of $\delta_{j,k}(t)$ implies that the model of each UAV needs more dissemination steps to be globally converged. The following remark shows that $\delta_k(t)$ is upper bounded throughout the whole training process.

Remark 2: There exists a constant δ_{max} *such that* $\delta_k(t) \leq \delta_{max}$, $\forall t \in T, k \in \mathcal{K}$. *At any iteration t, the dissemination gap of the farthest UAV (i.e., the UAV at the network edge),* $\delta_{max} = \alpha$ *gives a maximal value for the steps that the models of other UAVs have been disseminated to UAV k.*

Given the aforementioned analysis, we are now ready to prove the convergence of FedMoD.

Therorem 3: If the learning rate λ *satisfies* $1-\lambda L \geq 0$, $1-2\lambda^2L^2 > 0$, *we have*

$$\mathbb{E}[\|\nabla F(\tilde{\mathbf{u}})(t)\|_2^2] \leq \frac{2\{\mathbb{E}[F(\tilde{\mathbf{u}})(0) - F(\tilde{\mathbf{u}})(T)]\}}{\delta} + \lambda L\sum_{u=1}^{U_{inv}} m_u\sigma^2 \tag{21}$$

Proof: From (20), we have

$$\frac{\lambda}{2}\mathbb{E}\|\nabla F(\tilde{\mathbf{u}}(t))\|_2^2 \leq \mathbb{E}[F(\tilde{\mathbf{u}}(t))] - \mathbb{E}[F(\tilde{\mathbf{u}}(t+1))] + \frac{\lambda^2 L}{2}\sum_{u=1}^{U_{inv}} m_u\sigma^2 - \frac{\lambda}{2}(1-\lambda L)\tilde{Q}. \tag{22}$$

$$\mathbb{E}\|\nabla F(\tilde{\mathbf{u}}(t))\|^2 \leq \frac{2\{\mathbb{E}[F(\tilde{\mathbf{u}}(t))] - \mathbb{E}[F(\tilde{\mathbf{u}}(t+1))]\}}{\lambda} + \lambda L\sum_{i=1}^{U_{inv}} m_u\sigma^2 - (1-\lambda L)\tilde{Q} \tag{23}$$

Since $1-\lambda L \geq 0$ from Theorem 3, the third term in the RHS of (23) is eliminated, thus we have

$$\mathbb{E}[\|\nabla F(\tilde{\mathbf{u}})(t)\|_2^2] \leq \frac{2\{\mathbb{E}[F(\tilde{\mathbf{u}})(0) - F(\tilde{\mathbf{u}})(T)]\}}{\lambda} + \lambda L\sum_{u=1}^{U_{inv}} m_u\sigma^2 \tag{24}$$

■

APPENDIX C
PROOF OF LEMMA 1

By applying the global loss function to both sides of (19) and using the L-smoothness assumption, we have:

$$\begin{aligned}
&\mathbb{E}[F(\tilde{\mathbf{u}}(t+1))] \\
&\leq \mathbb{E}[F(\tilde{\mathbf{u}}(t))] + \mathbb{E}\left\langle \nabla F(\tilde{\mathbf{u}}(t)), -\lambda\mathbf{G}(t)\mathbf{m}\right\rangle \\
&\quad + \frac{L}{2}\mathbb{E}\|\lambda\mathbf{G}(t)\mathbf{m}\|_2^2 = \mathbb{E}[F(\tilde{\mathbf{u}}(t))] \\
&\quad - \delta\mathbb{E}\left\langle \nabla F(\tilde{\mathbf{u}}(t)), \mathbb{E}[\mathbf{G}(t)\mathbf{m}]\right\rangle \\
&\quad + \frac{\lambda^2 L}{2}\mathbb{E}\left\|\mathbf{G}(t)\mathbf{m} - \nabla\tilde{\mathbf{F}}(t)\mathbf{m} + \nabla\tilde{\mathbf{F}}(t)\mathbf{m}\right\|_2^2,
\end{aligned}$$

where $\nabla\tilde{\mathbf{F}}(t) = \left[\nabla F_1(t), \nabla F_2(t), \cdots, \nabla F_{U_{inv}}(t)\right]$. Since $\mathbb{E}[\hat{\mathbf{L}}(\tilde{\mathbf{w}}_i(t-y))\hat{\mathbf{m}}] = \nabla\tilde{\mathbf{L}}(\tilde{\mathbf{w}}_i(t-y))\hat{\mathbf{m}}$, we have the following

$$\begin{aligned}
&\mathbb{E}[F(\tilde{\mathbf{u}}(t+1))] \\
&= \mathbb{E}[F(\tilde{\mathbf{u}}(t))] - \lambda\mathbb{E}\left\langle \nabla F(\tilde{\mathbf{u}}(t)), \nabla\tilde{\mathbf{F}}(t)\mathbf{m}\right\rangle \\
&\quad + \frac{\lambda^2 L}{2}\mathbb{E}\left\|\mathbf{G}(t)\mathbf{m} - \nabla\tilde{\mathbf{F}}(t)\mathbf{m}\right\|_2^2 + \frac{\lambda^2 L}{2}\|\nabla\tilde{\mathbf{F}}(t)\mathbf{m}\|_2^2,
\end{aligned}$$

where $\frac{\lambda^2 L}{2}\mathbb{E}\left\|\mathbf{G}(t)\mathbf{m} - \nabla\tilde{\mathbf{F}}(t)\mathbf{m} + \nabla\tilde{\mathbf{F}}(t)\mathbf{m}\right\|_2^2 = \frac{\lambda^2 L}{2}\mathbb{E}\left\|\mathbf{G}(t)\mathbf{m} - \nabla\tilde{\mathbf{F}}(t)\mathbf{m}\right\|_2^2 + \frac{\lambda^2 L}{2}\mathbb{E}\|\nabla\tilde{\mathbf{F}}(t)\mathbf{m}\|_2^2$. This is becasue $\mathbb{E}[\mathbf{G}(t)\mathbf{m}] = \nabla\tilde{\mathbf{F}}(t)\mathbf{m}$, thus the cross-terms of $\mathbf{G}(t)\mathbf{m}$ and $\nabla\tilde{\mathbf{F}}(t)\mathbf{m}$ are zero. Thus, we have

$$\begin{aligned}
&\mathbb{E}[F(\tilde{\mathbf{u}}(t+1))] \\
&= \mathbb{E}[F(\tilde{\mathbf{w}}(t))] - \delta\mathbb{E}\left\langle \nabla F(\tilde{\mathbf{u}}(t)), \sum_{u=1}^{N_{inv}} m_u\nabla F_u(\tilde{\mathbf{u}}_u(t))\right\rangle \\
&\quad + \frac{\lambda^2 L}{2}\mathbb{E}\left\|\sum_{u=1}^{U_{inv}} m_u\Big(g(\tilde{\mathbf{u}}_u(t)) - \nabla F(\tilde{\mathbf{w}}_u(t))\Big)\right\|_2^2 \\
&\quad + \frac{\lambda^2 L}{2}\|\nabla\tilde{\mathbf{F}}(t)\mathbf{m}\|_2^2
\end{aligned}$$

$$= \mathbb{E}[F(\tilde{\mathbf{u}}(t))] - \lambda \mathbb{E}\left\langle \nabla F(\tilde{\mathbf{u}}(t)), \sum_{u=1}^{U_{inv}} m_u \nabla F_i(\tilde{\mathbf{w}}_u(t)) \right\rangle$$
$$+ \frac{\lambda^2 L}{2} \sum_{u=1}^{U_{inv}} m_u^2 \mathbb{E}\left\| g(\tilde{\mathbf{w}}_u(t)) - \nabla F_u(\tilde{\mathbf{w}}_u(t)) \right\|_2^2$$
$$+ \frac{\lambda^2 L}{2} \|\nabla \tilde{\mathbf{F}}(t)\mathbf{m}\|_2^2.$$

From Assumption 3, we have $\mathbb{E}\left\| g(\tilde{\mathbf{w}}_u(t)) - \nabla F_u(\tilde{\mathbf{w}}_u(t)) \right\|_2^2 \leq \sigma^2$. Also, $\mathbf{s}^T \mathbf{k} = \frac{1}{2}\|\mathbf{s}\|_2^2 + \frac{1}{2}\|\mathbf{k}\|_2^2 - \frac{1}{2}\|\mathbf{s}-\mathbf{k}\|_2^2$. Thus, we have

$$\lambda \mathbb{E}\left\langle \nabla F(\tilde{\mathbf{u}}(t)), \sum_{u=1}^{U_{inv}} m_u \nabla F_u(\tilde{\mathbf{w}}_u(t)) \right\rangle$$
$$= \frac{\lambda}{2} \|\nabla F(\tilde{\mathbf{u}}(t))\|_2^2$$
$$+ \frac{\lambda}{2} \mathbb{E}\|\sum_{u=1}^{U_{inv}} m_u \nabla F(\tilde{\mathbf{w}}_u(t))\|_2^2$$
$$- \frac{\lambda}{2} \mathbb{E}\left\| \nabla F(\tilde{\mathbf{u}}(t)) - \sum_{u=1}^{U_{inv}} m_u \nabla F(\tilde{\mathbf{w}}_u(t)) \right\|_2^2.$$

With such a constraint, we can have

$$\mathbb{E}[F(\tilde{\mathbf{u}}(t+1))]$$
$$\leq \mathbb{E}[F(\tilde{\mathbf{u}}(t))] - \Bigg(\frac{\lambda}{2} \|\nabla F(\tilde{\mathbf{u}}(t))\|_2^2$$
$$+ \frac{\lambda}{2} \mathbb{E}\left\| \sum_{u=1}^{U_{inv}} m_u \nabla F(\tilde{\mathbf{u}}_u(t)) \right\|_2^2 - \frac{\lambda}{2} \mathbb{E}\Bigg\| \nabla F(\tilde{\mathbf{u}}(t))$$
$$- \sum_{u=1}^{U_{inv}} m_u \nabla F(\tilde{\mathbf{w}}_i(t)) \Bigg\|_2^2 \Bigg)$$
$$+ \frac{\lambda^2 L}{2} \sum_{u=1}^{U_{inv}} m_u^2 \sigma^2 + \frac{\lambda^2 L}{2} \|\nabla \tilde{\mathbf{F}}(t)\mathbf{m}\|_2^2$$
$$\leq \mathbb{E}[F(\tilde{\mathbf{u}}(t))] - \Bigg(\frac{\lambda}{2} \|\nabla F(\tilde{\mathbf{u}}(t))\|_2^2 + \frac{\lambda}{2} \mathbb{E}\left\| \sum_{u=1}^{U_{inv}} m_u \nabla F(\tilde{\mathbf{w}}_u(t)) \right\|_2^2$$
$$- \frac{\lambda}{2} \mathbb{E}\left\| \sum_{u=1}^{U_{inv}} m_u \Big(\nabla F(\tilde{\mathbf{u}}(t)) - \nabla F(\tilde{\mathbf{w}}_u(t)) \Big) \right\|_2^2 \Bigg)$$
$$+ \frac{\lambda^2 L}{2} \sum_{u=1}^{U_{inv}} m_u^2 \sigma^2 + \frac{\lambda^2 L}{2} \mathbb{E}\|\nabla \sum_{u=1}^{U_{inv}} m_u \nabla F_u(\tilde{\mathbf{w}}_u(t))\|_2^2.$$

We denote $\tilde{Q} = \mathbb{E}\|\nabla \sum_{i=1}^{U_{inv}} m_u \nabla F_u(\tilde{\mathbf{w}}_u(t))\|_2^2$, we have the following

$$\mathbb{E}[F(\tilde{\mathbf{u}}(t+1))]$$
$$\leq \mathbb{E}[F(\tilde{\mathbf{u}}(t))] - \frac{\lambda}{2} \|\nabla F(\tilde{\mathbf{u}}(t))\|_2^2 - \left(\frac{\lambda}{2} - \frac{\lambda^2 L}{2} \right) \tilde{Q}$$
$$+ \frac{\lambda}{2} \mathbb{E}\left\| \sum_{u=1}^{U_{inv}} m_u \Big(\nabla F(\tilde{\mathbf{u}}(t)) - \nabla F(\tilde{\mathbf{w}}_u(t)) \Big) \right\|_2^2$$
$$+ \frac{\lambda^2 L}{2} \sum_{u=1}^{U_{inv}} m_u^2 \sigma^2$$
$$= \mathbb{E}[F(\tilde{\mathbf{u}}(t))] - \frac{\lambda}{2} \|\nabla F(\tilde{\mathbf{u}}(t))\|_2^2 - \left(\frac{\lambda}{2} - \frac{\lambda^2 L}{2} \right) \tilde{Q}$$
$$+ \frac{\lambda}{2} \mathbb{E}\left\| \sum_{u=1}^{U_{inv}} m_u \mathbb{E}\left\| \nabla F(\tilde{\mathbf{u}}(t)) - \nabla F(\tilde{\mathbf{w}}_i(t)) \right\| \right\|$$
$$+ \frac{\lambda^2 L}{2} \sum_{u=1}^{U_{inv}} m_u^2 \sigma^2$$
$$\leq \mathbb{E}[F(\tilde{\mathbf{u}}(t))] - \frac{\lambda}{2} \|\nabla F(\tilde{\mathbf{u}}(t))\|_2^2 - \left(\frac{\lambda}{2} - \frac{\lambda^2 L}{2} \right) \tilde{Q}$$
$$+ \frac{\lambda}{2} \mathbb{E}\left\| \sum_{u=1}^{U_{inv}} m_u \mathbb{E}\left\| \tilde{\mathbf{u}}(t) - \tilde{\mathbf{w}}_u(t) \right\| \right\| + \frac{\lambda^2 L}{2} \sum_{u=1}^{U_{inv}} m_u^2 \sigma^2.$$

The last inequality holds because of the L- smoothness assumption of the local loss function. We conclude the proof by moving $\mathbb{E}[F(\tilde{\mathbf{u}}(t))]$ to the left hand side (LHS), thus we will have

$$\begin{aligned} &\mathbb{E}[F(\tilde{\mathbf{u}}(t+1))] - \mathbb{E}[F(\tilde{\mathbf{u}}(t))] \\ &\quad \leq \frac{-\lambda}{2} \mathbb{E}\|\nabla F(\tilde{\mathbf{u}}(t))\|_2^2 \\ &\qquad + \frac{\lambda^2 L}{2} \sum_{u=1}^{U_{inv}} m_u \sigma^2 - \frac{\lambda}{2}(1 - \lambda L)\tilde{Q} \\ &\qquad + \frac{\lambda L^2}{2} \mathbb{E}\left\| \tilde{\mathbf{w}}(t)(\mathbf{I} - \mathbf{M}) \right\|_{\mathbf{M}}^2. \end{aligned} \tag{25}$$

REFERENCES

[1] L. Godage, "Global unmanned aerial vehicle market (UAV) industry analysis and forecast (2018–2026)," Mont. Ledger, Boston, MA, USA, Tech. Rep., 2018.

[2] M. Z. Hassan, G. Kaddoum, and O. Akhrif, "Interference management in cellular-connected Internet of Drones networks with drone-pairing and uplink rate-splitting multiple access," *IEEE Internet Things J.*, vol. 9, no. 17, pp. 16060–16079, Sep. 2022.

[3] S. Zhang, Y. Zeng, and R. Zhang, "Cellular-enabled UAV communication: A connectivity-constrained trajectory optimization perspective," *IEEE Trans. Commun.*, vol. 67, no. 3, pp. 2580–2604, Mar. 2019.

[4] *Technical Specification Group Services and System Aspects; Unmanned Aerial System (UAS) Support in 3GPP (Release 17)*, Standard 3GPP TS 22.125, 3rd Generation Partnership Project, Dec. 2019. [Online]. Available: https://www.3gpp.org/ftp/Specs/archive/22series/22.125/

[5] Z. Xiao et al., "Enabling UAV cellular with millimeter-wave communication: Potentials and approaches," *IEEE Commun. Mag.*, vol. 54, no. 5, pp. 66–73, May 2016.

[6] B. McMahan et al., "Communication-efficient learning of deep networks from decentralized data," in *Proc. 20th Int. Conf. Artif. Intell. Statist.*, 2017, pp. 1273–1282.

[7] S. Niknam, H. S. Dhillon, and J. H. Reed, "Federated learning for wireless communications: Motivation, opportunities, and challenges," *IEEE Commun. Mag.*, vol. 58, no. 6, pp. 46–51, Jun. 2020.

[8] Y. Qu et al., "Decentralized federated learning for UAV networks: Architecture, challenges, and opportunities," *IEEE Netw.*, vol. 35, no. 6, pp. 156–162, Dec. 2021.

[9] P. Chhikara, R. Tekchandani, N. Kumar, M. Guizani, and M. M. Hassan, "Federated learning and autonomous UAVs for hazardous zone detection and AQI prediction in IoT environment," *IEEE Internet Things J.*, vol. 8, no. 20, pp. 15456–15467, Oct. 2021.

[10] A. S. Abdalla and V. Marojevic, "Communications standards for unmanned aircraft systems: The 3GPP perspective and research drivers," *IEEE Commun. Standards Mag.*, vol. 5, no. 1, pp. 70–77, Mar. 2021.

[11] W. Y. B. Lim et al., "UAV-assisted communication efficient federated learning in the era of the artificial intelligence of things," *IEEE Netw.*, vol. 35, no. 5, pp. 188–195, Sep. 2021.

[12] C. B. Issaid, A. Elgabli, and M. Bennis, "Local stochastic ADMM for communication-efficient distributed learning," in *Proc. IEEE Wireless Commun. Netw. Conf. (WCNC)*, Austin, TX, USA, Apr. 2022, pp. 1880–1885.

[13] M. M. Wadu, S. Samarakoon, and M. Bennis, "Joint client scheduling and resource allocation under channel uncertainty in federated learning," *IEEE Trans. Commun.*, vol. 69, no. 9, pp. 5962–5974, Sep. 2021.

[14] M. Chen, Z. Yang, W. Saad, C. Yin, H. V. Poor, and S. Cui, "A joint learning and communications framework for federated learning over wireless networks," *IEEE Trans. Wireless Commun.*, vol. 20, no. 1, pp. 269–283, Jan. 2021.

[15] M. Chen, H. V. Poor, W. Saad, and S. Cui, "Convergence time optimization for federated learning over wireless networks," *IEEE Trans. Wireless Commun.*, vol. 20, no. 4, pp. 2457–2471, Apr. 2021.

[16] S. Wang et al., "Adaptive federated learning in resource constrained edge computing systems," *IEEE J. Sel. Areas Commun.*, vol. 37, no. 6, pp. 1205–1221, Jun. 2019.

[17] Z. Yang, M. Chen, W. Saad, C. S. Hong, and M. Shikh-Bahaei, "Energy efficient federated learning over wireless communication networks," *IEEE Trans. Wireless Commun.*, vol. 20, no. 3, pp. 1935–1949, Mar. 2021.

[18] J. Yao and N. Ansari, "Enhancing federated learning in fog-aided IoT by CPU frequency and wireless power control," *IEEE Internet Things J.*, vol. 8, no. 5, pp. 3438–3445, Mar. 2021.

[19] M. S. Al-Abiad, Md. Z. Hassan, and Md. J. Hossain, "Energy-efficient resource allocation for federated learning in NOMA-enabled and relay-assisted Internet of Things networks," *IEEE Internet Things J.*, vol. 9, no. 24, pp. 24736–24753, Dec. 2022.

[20] M. S. H. Abad, E. Ozfatura, D. Gunduz, and O. Ercetin, "Hierarchical federated learning across heterogeneous cellular networks," 2019, *arXiv:1909.02362*.

[21] L. Liu, J. Zhang, S. H. Song, and K. B. Letaief, "Client-Edge-Cloud hierarchical federated learning," in *Proc. IEEE Int. Conf. Commun. (ICC)*, Jun. 2020, pp. 1–6.

[22] S. Hosseinalipour, C. G. Brinton, V. Aggarwal, H. Dai, and M. Chiang, "From federated to fog learning: Distributed machine learning over heterogeneous wireless networks," *IEEE Commun. Mag.*, vol. 58, no. 12, pp. 41–47, Dec. 2020.

[23] S. Luo, X. Chen, Q. Wu, Z. Zhou, and S. Yu, "HFEL: Joint edge association and resource allocation for cost-efficient hierarchical federated edge learning," *IEEE Trans. Wireless Commun.*, vol. 19, no. 10, pp. 6535–6548, Oct. 2020.

[24] S. Liu, G. Yu, X. Chen, and M. Bennis, "Joint user association and resource allocation for wireless hierarchical federated learning with IID and non-IID data," *IEEE Trans. Wireless Commun.*, vol. 21, no. 10, pp. 7852–7866, Oct. 2022.

[25] F. P. Lin, S. Hosseinalipour, S. S. Azam, C. G. Brinton, and N. Michelusi, "Semi-decentralized federated learning with cooperative D2D local model aggregations," *IEEE J. Sel. Areas Commun.*, vol. 39, no. 12, pp. 3851–3869, Dec. 2021.

[26] Y. Sun, J. Shao, Y. Mao, J. Hui Wang, and J. Zhang, "Semi-decentralized federated edge learning for fast convergence on non-IID data," 2021, *arXiv:2104.12678*.

[27] Y. Sun, J. Shao, Y. Mao, J. H. Wang, and J. Zhang, "Semi-decentralized federated edge learning with data and device heterogeneity," 2021, *arXiv:2112.10313*.

[28] M. S. Al-Abiad and Md. J. Hossain, "Coordinated scheduling and decentralized federated learning using conflict clustering graphs in fog-assisted IoD networks," *IEEE Trans. Veh. Technol.*, vol. 72, no. 3, pp. 3455–3472, Mar. 2023.

[29] M. Akbari, A. Syed, W. S. Kennedy, and M. Erol-Kantarci, "Constrained federated learning for AoI-limited SFC in UAV-aided MEC for smart agriculture," *IEEE Trans. Mach. Learn. Commun. Netw.*, vol. 1, pp. 277–295, 2023.

[30] S. B. Azmy, A. Abutuleb, S. Sorour, N. Zorba, and H. S. Hassanein, "Optimal transport for UAV D2D distributed learning: Example using federated learning," in *Proc. IEEE Interfaces Conf. Commun. ICC*, Montreal, QC, Canada, 2021, pp. 1–6.

[31] R. Khelf, E. Driouch, and W. Ajib, "On the optimization of UAV-assisted wireless networks for hierarchical federated learning," in *Proc. IEEE 34th Annu. Int. Symp. Pers., Indoor Mobile Radio Commun. (PIMRC)*, Toronto, ON, Canada, 2023, pp. 1–6.

[32] A. Douik, H. Dahrouj, T. Y. Al-Naffouri, and M. Alouini, "Distributed hybrid scheduling in multi-cloud networks using conflict graphs," *IEEE Trans. Commun.*, vol. 66, no. 1, pp. 209–224, Jan. 2018.

[33] M. S. Al-Abiad, M. Obeed, M. J. Hossain, and A. Chaaban, "Decentralized aggregation for energy-efficient federated learning via d2d communications," *IEEE Trans. Commun.*, vol. 71, no. 6, pp. 3333–3351, Jun. 2023.

[34] J. Sabzehali, V. K. Shah, H. S. Dhillon, and J. H. Reed, "3D placement and orientation of mmWave-based UAVs for guaranteed LoS coverage," *IEEE Wireless Commun. Lett.*, vol. 10, no. 8, pp. 1662–1666, Aug. 2021.

[35] N. Cherif, M. Alzenad, H. Yanikomeroglu, and A. Yongacoglu, "Downlink coverage and rate analysis of an aerial user in vertical heterogeneous networks (VHetNets)," *IEEE Trans. Wireless Commun.*, vol. 20, no. 3, pp. 1501–1516, Mar. 2021.

[36] M. Mozaffari, W. Saad, M. Bennis, and M. Debbah, "Efficient deployment of multiple unmanned aerial vehicles for optimal wireless coverage," *IEEE Commun. Lett.*, vol. 20, no. 8, pp. 1647–1650, Aug. 2016.

[37] V. V. Chetlur and H. S. Dhillon, "Coverage and rate analysis of downlink cellular vehicle-to-everything (C-V2X) communication," *IEEE Trans. Wireless Commun.*, vol. 19, no. 3, pp. 1738–1753, Mar. 2020.

[38] M. B. Ghorbel et al., "Joint position and travel path optimization for energy efficient wireless data gathering using unmanned aerial vehicles," *IEEE Trans. Veh. Technol.*, vol. 68, no. 3, pp. 2165–2175, Mar. 2019.

[39] A. P. Chandrakasan, S. Sheng, and R. W. Brodersen, "Low-power CMOS digital design," *IEEE J. Solid-State Circuits*, vol. 27, no. 4, pp. 473–484, Apr. 1992.

[40] T. D. Burd and R. W. Brodersen, "Processor design for portable systems," *J. VLSI Signal Process. Syst. Signal, Image Video Technol.*, vol. 13, no. 2–3, pp. 203–221, 1996.

[41] H. Ghazzai, M. B. Ghorbel, A. Kadri, M. J. Hossain, and H. Menouar, "Energy-efficient management of unmanned aerial vehicles for underlay cognitive radio systems," *IEEE Trans. Green Commun. Netw.*, vol. 1, no. 4, pp. 434–443, Dec. 2017.

MOHAMMED SAIF (Member, IEEE) received the B.Sc. degree in computer and communications engineering from Taiz University, Taiz, Yemen, in 2010, the M.Sc. degree in electrical engineering from the King Fahd University of Petroleum and Minerals, Dhahran, Saudi Arabia, in 2017, and the Ph.D. degree in electrical engineering from The University of British Columbia, Kelowna, BC, Canada, in 2020. He is currently a Post-Doctoral Research Fellow with the Department of Electrical and Computer Engineering, University of Toronto, Toronto, Canada. Prior to that, he was a Post-Doctoral Research Fellow with the School of Engineering, The University of British Columbia, Canada, from 2020 to 2022. His research interests include optimization and wireless communications, federated learning, MIMO radar, and massive connectivity of multi-RIS-assisted UAV communications. He was a recipient of the Natural Science and Engineering Research Council Postdoctoral Fellowship (NSERC PDF) of Canada in 2023.

MD. ZOHEB HASSAN (Member, IEEE) received the Ph.D. degree from the Department of Electrical and Computer Engineering, The University of British Columbia, Vancouver, BC, Canada. He is currently an Assistant Professor with the Department of Electrical and Computer Engineering, Université Laval, Canada. Prior to joining Université Laval, he was a Senior Post-Doctoral Research Fellow with École de technologie superiéure (ETS) and a Research Assistant Professor with the Department of Electrical and Computer Engineering, Virginia Tech, USA. He has authored and coauthored over 30 journal articles and 15 conference papers in radio resource optimization, interference management, spectrum sharing, and optical wireless communications. He has served/is serving as a TPC member for various prestigious IEEE conferences, such as IEEE GLOBECOM, ICC, MILCOM, VTC, and PIMRC. He was a recipient of the NSERC Postdoctoral Fellowship Award in 2021 and the Four-Year Fellowship from the University of British Columbia in 2014. He is a reviewer of several major journals of the IEEE Communication Society.

MD. JAHANGIR HOSSAIN (Senior Member, IEEE) received the B.Sc. degree in electrical and electronics engineering from Bangladesh University of Engineering and Technology (BUET), Dhaka, Bangladesh, the M.A.Sc. degree from the University of Victoria, Victoria, BC, Canada, and the Ph.D. degree from The University of British Columbia (UBC), Vancouver, BC. He was a Lecturer with BUET. He was a Research Fellow with McGill University, Montreal, QC, Canada; the National Institute of Scientific Research, Quebec, QC; and the Institute for Telecommunications Research, University of South Australia, Mawson Lakes, SA, Australia. His industrial experience includes a Senior Systems Engineer position with Redline Communications, Markham, ON, Canada, and a Research Intern position with the Communication Technology Laboratory, Intel Inc., Hillsboro, OR, USA. He is currently a Professor with the School of Engineering, UBC Okanagan Campus, Kelowna, BC. His research interests include designing spectrally and power-efficient modulation schemes, applications of machine learning for communications, quality-of-service issues and resource allocation in wireless networks, and optical wireless communications. He regularly serves as a member of the Technical Program Committee for the IEEE International Conference on Communications (ICC) and the IEEE Global Telecommunications Conference (GLOBECOM). He is serving as an Editor for IEEE TRANSACTIONS ON COMMUNICATIONS. He previously served as an Editor for IEEE TRANSACTIONS ON WIRELESS COMMUNICATIONS and an Associate Editor for IEEE COMMUNICATIONS SURVEYS AND TUTORIALS.